Science of the Total Environment 866 (2023) 161220

Contents lists available at ScienceDirect

Science of the Total Environment

journal homepage: www.elsevier.com/locate/scitotenv

Towards European automatic bioaerosol monitoring: Comparison of 9 automatic pollen observational instruments with classic Hirst-type traps

José M. Maya-Manzano [a,1], Fiona Tummon [b], Reto Abt [c], Nathan Allan [d], Landon Bunderson [d], Bernard Clot [b], Benoît Crouzy [b], Gintautas Daunys [e], Sophie Erb [b], Mónica Gonzalez-Alonso [f,2], Elias Graf [c], Łukasz Grewling [g], Jörg Haus [h], Evgeny Kadantsev [i], Shigeto Kawashima [j], Moises Martinez-Bracero [k,3], Predrag Matavulj [l], Sophie Mills [m], Erny Niederberger [c], Gian Lieberherr [b], Richard W. Lucas [d], David J. O'Connor [n], Jose Oteros [o], Julia Palamarchuk [i], Francis D. Pope [m], Jesus Rojo [p], Ingrida Šaulienė [e], Stefan Schäfer [h], Carsten B. Schmidt-Weber [a], Martin Schnitzler [h], Branko Šikoparija [l], Carsten A. Skjøth [q,r], Mikhail Sofiev [i], Tom Stemmler [h], Marina Triviño [a,4], Yanick Zeder [c], Jeroen Buters [a,*]

[a] Center of Allergy & Environment (ZAUM), Member of the German Center for Lung Research (DZL), Technical University and Helmholtz Center Munich, Munich, Germany
[b] Federal Office of Meteorology and Climatology (MeteoSwiss), Payerne, Switzerland
[c] Swisens AG, Horw, Switzerland
[d] Pollen Sense TM, UT, USA
[e] Šiauliai Academy, Vilnius University, Šiauliai, Lithuania
[f] Department of Environmental Biology, University of Navarra, Pamplona, Spain
[g] Laboratory of Aerobiology, Department of Systematic and Environmental Botany, Adam Mickiewicz University, Poznan, Poland
[h] Helmut Hund Wetzlar, Wetzlar, Germany
[i] Finnish Meteorological Institute, Helsinki, Finland
[j] Graduate School of Agriculture, Kyoto University, Kyoto, Japan
[k] Technological University Dublin, Dublin, Ireland
[l] BioSense Institute Research Institute for Information Technologies in Biosystems, University of Novi Sad, Novi Sad, Serbia
[m] School of Geography, Earth and Environmental Sciences, University of Birmingham, Birmingham, United Kingdom
[n] School of Chemical Sciences, Dublin City University, Dublin, Ireland
[o] Department of Botany, Ecology and Plant Physiology, University of Cordoba, Cordoba, Spain
[p] Department of Pharmacology, Pharmacognosy and Botany, Complutense University of Madrid, Madrid, Spain
[q] Department of Environmental Science, Aarhus University, Aarhus, Denmark
[r] School of Science and the Environment, University of Worcester, Worcester, United Kingdom

HIGHLIGHTS

GRAPHICAL ABSTRACT

* Corresponding author at: Center of Allergy & Environment (ZAUM), Member of the German Center for Lung Research (DZL), Technical University München/Helmholtz Center, Biedersteiner Str. 29, 80802 Munich, Germany.
E-mail addresses: jmmaya@unex.es (J.M. Maya-Manzano), fiona.tummon@meteoswiss.ch (F. Tummon), reto.abt@swisens.ch (R. Abt), nate@pollensense.com (N. Allan), landon@pollensense.com (L. Bunderson), bernard.clot@meteoswiss.ch (B. Clot), Benoit.Crouzy@meteoswiss.ch (B. Crouzy), Gintautas.daunys@sa.vu.lt (G. Daunys), Sophie.Erb@meteoswiss.ch (S. Erb), mgonzalez.23@alumni.unav.es (M. Gonzalez-Alonso), elias.graf@swisens.ch (E. Graf), J.Haus@hund.de (J. Haus), Evgeny.Kadantsev@fmi.fi (E. Kadantsev), sig@kais.kyoto-u.ac.jp (S. Kawashima), moises.martinezbracero@dcu.ie (M. Martinez-Bracero), matavulj.predrag@biosense.rs (P. Matavulj), SAM919@student.bham.ac.uk (S. Mills), erny.niederberger@swisens.ch (E. Niederberger), Gian-Duri.Lieberherr@meteoswiss.ch (G. Lieberherr), rich@pollensense.com (R.W. Lucas), david.x.oconnor@dcu.ie (D.J. O'Connor), b42otmoj@uco.es (J. Oteros), yuliia.palamarchuk@fmi.fi (J. Palamarchuk), F.Pope@bham.ac.uk (F.D. Pope), jesrojo@ucm.es (J. Rojo), ingrida.sauliene@sa.vu.lt (I. Šaulienė), S.Schaefer@hund.de (S. Schäfer), csweber@tum.de (C.B. Schmidt-Weber), M.Schnitzler@hund.de (M. Schnitzler), sikoparijabranko@biosense.rs (B. Šikoparija), Mikhail.Sofiev@fmi.fi (M. Sofiev), t.stemmler@hund.de (T. Stemmler), yanick.zeder@swisens.ch (Y. Zeder), buters@tum.de (J. Buters).
[1] Present address: Department of Plant Biology, Ecology and Earth Sciences (Botany area), Faculty of Sciences, University of Extremadura, Badajoz, Spain.
[2] Present address: Center of Allergy & Environment (ZAUM), Member of the German Center for Lung Research (DZL), Technical University and Helmholtz Center Munich, Munich, Germany.
[3] Present address: School of Chemical Sciences, Dublin City University, Dublin, Ireland.
[4] Present address: Agroforestry and Plant Biochemistry, Proteomics and Systems Biology, Department of Biochemistry and Molecular Biology, University of Cordoba, UCO-CeiA3, Cordoba, Spain.

http://dx.doi.org/10.1016/j.scitotenv.2022.161220
Received 27 October 2022; Received in revised form 15 December 2022; Accepted 23 December 2022
Available online 28 December 2022

- Daily results compared better with the Hirst observations than the 3-hourly values.
- For individual pollen types, results similar to the Hirst were frequently shown by a few systems.
- Automatic systems performed best for *Betula,* then *Quercus* and *Fraxinus*, while worst for Poaceae.
- Different algorithms applied to the same device also showed different results.
- Some automatic systems are capable of being used operationally to provide real time observations.

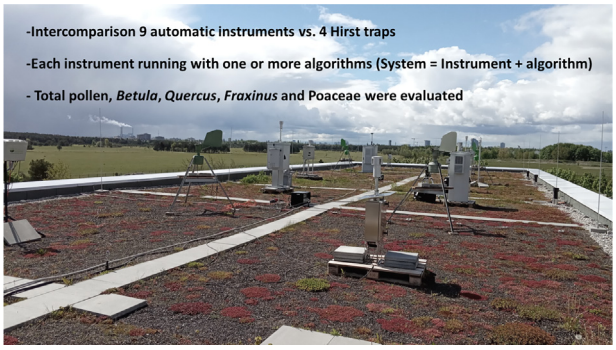

ARTICLE INFO

Guest Editor: Pavlos Kassomenos

Keywords:
Aerobiology
Automatic monitoring
Pollen classification
Intercomparison campaign
Pollen
Real-time

ABSTRACT

To benefit allergy patients and the medical practitioners, pollen information should be available in both a reliable and timely manner; the latter is only recently possible due to automatic monitoring. To evaluate the performance of all currently available automatic instruments, an international intercomparison campaign was jointly organised by the EUMETNET AutoPollen Programme and the ADOPT COST Action in Munich, Germany (March–July 2021).
The automatic systems (hardware plus identification algorithms) were compared with manual Hirst-type traps. Measurements were aggregated into 3-hourly or daily values to allow comparison across all devices. We report results for total pollen as well as for *Betula*, *Fraxinus*, Poaceae, and *Quercus*, for all instruments that provided these data. The results for daily averages compared better with Hirst observations than the 3-hourly values. For total pollen, there was a considerable spread among systems, with some reaching $R^2 > 0.6$ (3 h) and $R^2 > 0.75$ (daily) compared with Hirst-type traps, whilst other systems were not suitable to sample total pollen efficiently ($R^2 < 0.3$). For individual pollen types, results similar to the Hirst were frequently shown by a small group of systems. For *Betula*, almost all systems performed well ($R^2 > 0.75$ for 9 systems for 3-hourly data). Results for *Fraxinus* and *Quercus* were not as good for most systems, while for Poaceae (with some exceptions), the performance was weakest. For all pollen types and for most measurement systems, false positive classifications were observed outside of the main pollen season. Different algorithms applied to the same device also showed different results, highlighting the importance of this aspect of the measurement system. Overall, given the 30 % error on daily concentrations that is currently accepted for Hirst-type traps, several automatic systems are currently capable of being used operationally to provide real-time observations at high temporal resolutions. They provide distinct advantages compared to the manual Hirst-type measurements.

1. Introduction

Pollen is a major cause of allergies worldwide, affecting an estimated 10–30 % of the global population (World Allergy Organization, 2013). This is likely to worsen with climate change for most allergenic taxa as pollen concentrations continue to increase (Glick et al., 2021; Ziska et al., 2019), with longer pollen seasons, and earlier season start (Anderegg et al., 2021; Rojo et al., 2021a; Zhang and Steiner, 2022). Historically, pollen monitoring sites were mainly established to help diagnose and treat allergy sufferers (Bousquet et al., 2008). However, the sites and observations are also used for a wide range of other purposes, such as studying the impacts of climate change (Rojo et al., 2021a, 2021b), producing crop forecasts (Oteros et al., 2014), tracking invasive species and habitat shifts (Lake et al., 2017; Thibaudon et al., 2014), or for detecting pathogenic fungal spores (Isard et al., 2011). The majority of sites still use manual samplers (Buters et al., 2018) such as the Hirst-type pollen and spore trap (Hirst, 1952) or the Rotorod (Grinnellet al, 1961). Aerobiological networks have made real efforts to standardize the method used and to reduce bias to a minimum, with particular focus on the quality of counting as promoted by the International Association for Aerobiology (IAA) (Oteros et al., 2013; Galán et al., 2014; Sikoparija et al., 2017; Milic et al., 2019; Smith et al., 2019). The manual methods, although a major leap forward in pollen and spore monitoring at the time they were developed, have several drawbacks. For instance, although in some places the drum is daily replaced and the slides immediately counted to inform with the lower delay as possible (Bannister et al., 2021), usually the information provided by these devices is available with a delay of between 1 and 9 days as a result of the manual counting process. The data are mostly available only as daily averages, in part because of logistical and budget restraints related to obtaining data at higher resolutions, but also because of the high level of uncertainty associated with the low sampling rate (Adamov et al., 2021). Other uncertainties stem from fluctuations in the airflow (Oteros et al., 2017), the methodology chosen for counting (Sikoparija et al., 2011), differences between adhesives (Galán and Domínguez-Vilches, 1997; Maya-Manzano et al., 2018), and also between pollen counters (Sikoparija et al., 2017; Oteros et al., 2020). Despite these disadvantages, Hirst-type traps are currently the only base against which other devices can be compared in terms of pollen and fungal spore counts.

Over the past few years, a number of devices capable of detecting pollen and other bioaerosols in real-time have emerged, using a wide spectrum of different approaches (Buters et al., 2022; Huffman et al., 2020). This includes the KH-3000 (Kawashima et al., 2017; Kawashima et al., 2007); the family of Wideband Integrated Bioaerosol Spectrometer (WIBS) instruments (Healy et al., 2014; O'Connor et al., 2014) with its latest model, the WiBS-NEO/5 (Hughes et al., 2020); the BAA500 (Oteros et al., 2020; Oteros et al., 2015; Plaza et al., 2022); the PA-300 (Crouzy et al., 2016) and its successor, the Rapid E (Šaulienė et al., 2019; Tešendić et al., 2020); the SwisensPoleno (Sauvageat et al., 2020; Sofiev et al., 2022) and the Automated PollenSense (Jiang et al., 2022). Technologies and methods are evolving rapidly and new instruments are continuously being developed.

To evaluate all currently available commercial instruments and research prototypes, an international intercomparison was organised under the auspices of the EUMETNET AutoPollen Programme and the ADOPT COST Action (CA18226). The campaign provided a neutral, fair, and transparent assessment of the performance of a large number of different instruments since all measurements were carried out under the same environmental conditions (meteorology, surrounding land use and

vegetation) and with all instruments run by a completely independent operator. The main aims were (1) to evaluate the performance of all available bioaerosol monitors, particularly those with the capacity to identify pollen and/or fungal spores in real-time; (2) to work together with instrument manufacturers and researchers to provide feedback and encourage further development; and (3) to build capacity and share experience across the community working with and developing these real-time monitors. In addition to the large range of automatic instruments, four manual Hirst-type traps were run in parallel to provide a baseline against which to evaluate the automatic devices. The campaign was considerably more extensive in terms of the number of participating instruments compared to a campaign carried out in Payerne, Switzerland, in 2019 (Tummon et al., 2021). Moreover, it also established a set of good practices to be considered in any future evaluation of real-time bioaerosol monitoring devices (Clot et al., 2020).

2. Material and methods

2.1. Campaign site

The EUMETNET AutoPollen-COST ADOPT campaign was held in Munich, southern Germany, from 3 March to 14 July 2021. The site is located at 519 m above sea level in a region with a climate classified as continental with warm summers (category Cfb; Kottek et al., 2006). All devices were installed on the rooftop of the Biorepository building at the Helmholtz Zentrum München, which is located to the north of the city (11.5956°E, 48.2208° N; Supplementary material, Fig. S1). The rooftop is 10.5 m above the surrounding ground, a height shown to provide representative sampling (Rojo et al., 2019a). To minimize possible disturbance by turbulence, all monitors were placed at a distance of 4 m from each other and 3 m away from the edge of the building. The height of the inlets was slightly variable but mostly >1.8 m above the surface of the rooftop, including for the Hirst traps. All data were formatted to CET time. A more complete description of the surrounding vegetation, the meteorology during the campaign, and the manual Hirst observations is provided by Triviño et al. (2023).

2.2. Campaign logistics and regulations

To ensure complete transparency, once all devices were installed the instrument providers had no access to their devices for the duration of the campaign. The only exception was given for the PollenSense monitor (see below), which required internet access to run the algorithm used to classify pollen types. Monitoring was carried out centrally by an independent operator and any warnings were sent to instrument providers separately. When access to a device was required, temporary remote access was provided and any actions taken logged.

The manual pollen counts were carried out by two independent counters belonging to a group that had no link to any of the devices. Hirst data were not released to any of the participants until they had submitted the time series from the automatic instrument(s) to ensure a completely blind production of datasets from all real-time devices.

Three instruments (a Plair Rapid-E, a SwisensPoleno Neptune, and a Yamatronics KH-3000) were calibrated using polystyrene latex spheres at the Swiss Federal Institute of Metrology METAS to assess counting efficiency both before and after the main campaign (following the method applied in Lieberherr et al., 2021). These tests were carried out for a range of particle sizes (1, 2, 5, 10, and 15 μm) to assess whether there was any drift in time in terms of counting efficiency over the campaign. Results from these analyses will be published in a companion paper.

2.3. Description of the instruments used in the campaign

The list of all participating instruments, their identification capabilities, and some technical details are provided in Table 1 and in the following paragraphs (for further information see Buters et al. (2022)). Table S1 lists the devices for which data were analysed. A few additional prototypes and particle detectors were also run during the campaign, however the results from these instruments are not presented here.

2.3.1. Manual Hirst-type traps

Four Hirst-type volumetric traps (all Burkard models), called A, B, C and D, were installed and run following the European standard method (EN16828:2020). The airflow for each was set to 10 L/min using hand-held rotameters, but their flow was later mathematically corrected during analysis using measurements from resistance-free flowmeters (further described in Triviño et al., 2023, *submitted*). The average resistance-free flowrate for the traps was 14.4 ± 0.3 L/min for A, 13.4 ± 0.3 L/min for B, 13.2 ± 0.3 L/min for C, and 13.4 ± 0.3 L/min for D. Due to malfunctions, data from trap A is only available from 24 March onwards and from trap B from 31 March until the end of the campaign (14 July). Traps C and D worked continuously from the beginning (3 March) until the end. Four longitudinal scans were counted at 400× magnification, representing 15.8 % of the total surface area of each slide. This follows the recommendations (at least 10 %) of the European standard EN 16868:2020. Further details regarding the Hirst observations are provided by Triviño et al. (2023). The pollen taxa that were counted and how the total pollen was calculated are presented in Table S2 (Supplementary material).

2.3.2. Alphasense optical particle counter N3

The Alphasense Optical Particle Counter (OPC) N3 detects particles with diameters ranging between 0.35 and 40 μm (spherical equivalent size) based on a refractive index of 1.5. The raw data output is 24 different particle size bins which record the number of particle counts detected in a given sample time (generally 5 s) for each size bin. Using the sample time period and flow rate (mL/s) provided, the raw bin counts were converted into particle concentrations (particles/m^3). Three Alphasense OPC-N3s were run for the duration of the campaign, with the mean of all devices for which data was available presented. For this campaign, the flow was on average 5.2 L/min (range 1.5–7.5 L/min).

The sum of all concentrations of particles >10 μm in diameter was taken as a proxy for pollen in this study. This threshold thus likely also includes some fungal spores and large dust particles. Since the sampled air is not dried prior to measurement, these low-cost sensors have been shown to display a hygroscopic effect at high relative humidities, with the ratio of measured mass concentrations relative to reference instruments increasing exponentially at relative humidities above ~85 % (Crilley et al., 2018). A correction factor can be applied using κ-Köhler theory with appropriate humidity values, although it should be noted that no such correction was applied for this campaign. Instead, the data for episodes with precipitation >2 mm/h or for periods when relative humidity >70 % were set to zero.

2.3.3. Flir instantaneous bioaerosol analysis and Collection-2 (IBAC-2)

The Flir Instantaneous Bioaerosol Analysis and Collection-2 (IBAC-2) is the latest iteration of instruments previously known as the FIDO B2. The IBAC-2 uses light-induced fluorescence (LIF) to detect particles with diameters between 0.7 and 10 μm. It has a sample flow rate of 4 L/min and a time resolution of 1 s. It can potentially differentiate between biological and non-biological particles using a 405 nm laser to excite fluorescence (DeFreez, 2009; Flir IBAC-2, 2022). Should the emitted fluorescence (measured between 450 and 600 nm) exceed a pre-set threshold, a particle is deemed to be biological. The device can thus potentially detect pollen fragments, spores, bacteria and other biological aerosol particles in the range of 0.7–10 μm (DeFreez, 2009; Santarpia et al., 2013). It should be noted that individual particle data are not provided. Rather, particles are divided into four different groups based on both their size and fluorescence. Concentration values are thus available for the following categories: “small biological” (0.7–1.5 μm in size and fluorescent), “large biological” (1.5–10 μm in size and fluorescent), “small total” (all fluorescent and non-fluorescent particles in the size range 0.7–1.5 μm) and “large total” (all particles between 1.5 and 10 μm) (DeFreez, 2009; Santarpia et al., 2013; Jonsson and Kullander, 2014). In this study, the “large biological” category

Table 1
Data availability for each instrument over the duration the campaign (expressed in % of the total campaign time). Also the capabilities of each instrument are shown, according to literature.

Device	Data availability (%)	Instrument Type	Identification possibilities according to literature	Initial cost
Hirst A	81.4 %	Manual instrument	Pollen taxa	Low
Hirst B	72.6 %	Manual instrument	Pollen taxa	Low
Hirst C	100.0 %	Manual instrument	Pollen taxa	Low
Hirst D	100.0 %	Manual instrument	Pollen taxa	Low
Alphasense[1]	99.9 %	Design prototype	Particle counts	Low
ACPD TU Graz[2]	–	Design prototype	Pollen taxa	Low
CNRS Sextant[2]	–	Design prototype	Pollen taxa	Low
BAA500	99.1 %	Commercially-available	Pollen taxa, *Alternaria* spores	High
DMT WIBS[2]	–	Commercially-available	Particle counts and fluorescent particles	Moderate /High
IBAC-2[1]	73.1 %	Commercially-available	Particle counts and fluorescent particles	Low/Moderate
KH-3000	93.2 %	Commercially-available	Some pollen taxa	Low
Poleno Jupiter	100.0 %	Commercially-available	Pollen taxa, *Alternaria* spores	High
Poleno Mars	78.8 %	Commercially-available	Pollen taxa, *Alternaria* spores	High
Poleno Neptune	100.0 %	Commercially-available	Pollen taxa, *Alternaria* spores	High
PollenSense[1]	99.66 %	Commercially-available	Pollen taxa	Low
Rapid-E	100.0 %	Commercially-available	Pollen taxa	High

[1] For devices that were installed after the start date for the campaign (3 March 2021), data availability is calculated from the date of installation.
[2] ACPD TU Graz and CNRS Sextant did not cover a significant period of time within the campaign and were not included in further analysis. DMT WIBS decided not to participate in further analysis.

of particles was used as a proxy for pollen concentrations, with a similar rainfall filter applied as for the AlphaSense OPC-N3 (values with precipitation >2 mm/h were set to zero). It is important to note that as for all LIF-based instruments, the potential for anthropogenic particles to fluoresce in the same region as biological particles exists, and they may thus interfere with results (Santarpia et al., 2013).

The IBAC-2 was designed essentially as a bio-threat detection device and thus an additional gravimetric filter sampler (secondary sampling system) can be activated at a user-selected concentration threshold of fluorescent particles. These samples can later be analysed using off-line analytical methods (Jonsson and Kullander, 2014; Santarpia et al., 2013). This capacity was not used in this study.

2.3.4. Helmut Hund BAA500

The Helmut Hund BAA500 system uses automated optical microscopy in combination with digital image acquisition and recognition to identify pollen particles. The sampling unit is a virtual impactor and it samples a total volume of 1120 L/min for one minute every 10 min (adjustable). From this, 100 L/min is sampled with particles being deposited onto gel-covered sample carriers. Sampling is carried out for a period of three hours (adjustable to a minimum of 1 h) after which the carrier is shifted to a heating station where the impacting gel is briefly liquefied. This rehydrates the pollen grains present in the sample. The sample is then moved below a digital microscope for analysis. The microscope-camera photographs around 144 different areas in the carrier (about 33 % of the surface), and an image stack of each area is generated. Each image stack is made up of 180 images at different positions along the z-axis and is used to produce one 'synthetic' 2D image with increased depth of field. Subsequently, a segmentation algorithm identifies relevant image objects that are then analysed by a classification algorithm.

In this study, two different algorithms were applied. The original classification algorithm (BAA500-FIT) uses linear discriminant analysis based on classical, feature-based techniques. Although this algorithm has shown reliable results (Oteros et al., 2020; Plaza et al., 2022), the classification features have to be manually selected and adapted. A second, newer algorithm based on a convolutional neural network (CNN) (BAA500-AI) was developed and has to-date been tested on 20 pollen classes. Recently, the identification of *Alternaria* spores has also been reported (González-Alonso et al., 2022).

2.3.5. Plair rapid-E

The Plair Rapid-E cytometer samples air at a flowrate of 2.8 L/min. It uses a 405 nm laser to produce a time-resolved scattering signal which is measured by 24 detectors located at angles ranging from 45 to 135° from the laser beam. In addition, a LIF UV laser at 337 nm induces fluorescence that is measured across 32 channels from 350 to 800 nm. Eight sequential acquisitions at 500 ns intervals are taken while fluorescence lifetime is recorded in four spectral bands at 2 ns resolution (Šaulienė et al., 2019).

Three classification algorithms were applied in this study. Two algorithms developed by the BioSense Institute were based on all the above-mentioned data: scattering image, fluorescence spectrum, and fluorescence lifetime. Each input is processed with its own convolutional block, which consists of batch normalisation, convolutional layers, and a ReLu activation function. The data processing and network algorithm is described in detail by Tešendić et al. (2020). Reference data for training classification models were obtained from four different Rapid-E devices measuring in Novi Sad (Serbia), Osijek (Croatia), San Michele all'Adige (Italy), and Munich (Germany). i.e. measurements of known pollen of interest and for the class *other* (operational measurements from periods when no pollen were detected in the atmosphere). All training datasets were obtained using the device's proprietary "smart pollen mode" that, among others, filters out particles <8 μm in optical diameter (Šikoparija, 2020). The first classification model from BioSense Institute (Rapid-E BS) classified 16 pollen classes (*Alnus*, *Betula*, *Carpinus*, *Corylus*, *Fagus*, *Fraxinus*, *Plantago*, *Platanus*, Poaceae, *Populus*, *Quercus*, *Salix*, Taxaceae, *Tilia*, *Ulmus*, Urticaceae) and class *other* while the second model (Rapid-E V88 BS) classified 9 pollen classes (*Alnus*, *Betula*, *Carpinus*, *Corylus*, *Fraxinus*, *Pinus*, Poaceae, *Taxus*, Urtica) and *other*.

The third algorithm for the Plair Rapid-E was developed by Siauliai Academy of Vilnius University and the Finnish Meteorological Institute (FMI) and applied to the campaign by FMI (Rapid-E FMI). Prior to application of the identification algorithm, all non-fluorescent particles (signal intensity <1500 units) were filtered out. The Rapid-E FMI algorithm is based on a combination of two CNN, one each for the scattering image and fluorescence spectrum, although the architecture is identical for both types of signals: three convolutional blocks and three fully-connected layers (Šaulienė et al., 2019; Daunys et al., 2021). The lifetime signal was not included in the algorithm architecture due to its noisy characteristics and its negligible influence on recognition skill since very similar information is provided by the time-resolved fluorescence spectra (Šaulienė et al., 2019).

2.3.6. PollenSense automated particulate sensor

The PollenSense Automated Particle Sensor (APS) is an image-based automatic particle detector. Air is sucked in through an orifice at the bottom of the device at a rate of 13.7 L/min and particles impact onto a tape coated with adhesive that moves below the orifice at a rate of 68 mm/h. The camera has a 350× magnification and takes pictures once every 80 s. Images

are directly sent to the cloud where a classification algorithm analyses the images and assigns each particle to a class with a given probability score.

The APS algorithm was previously trained with data from a number of allergenic pollen species present in Europe (*Alnus glutinosa, Artemisia vulgaris, Betula* spp., *Corylus* spp., *Cupressus sempervirens, Poa pratensis*, and *Urtica dioica*). Two algorithms were used in this campaign (APS and APS VT60), with both using a CNN-based architecture (company's proprietary) (Jiang et al., 2022). The APS algorithm was trained using specimens collected in North America. The APS VT60 algorithm is an updated iteration of the APS algorithm, including training data collected from European pollen taxa.

2.3.7. Swisens Poleno

The Swisens Poleno instruments are real-time airflow cytometers that integrate different methods for in-flight particle observations. They measure uninterrupted and are operated at a constant airflow rate of 40 L/min. If a particle is detected, two holographic images (0.595 μm pixel resolution) are taken by means of digital inline holography. Subsequently, a fluorescence measurement is carried out with three different modulated LED light sources (280 nm, 365 nm, 405 nm), which excite the particle one after the other. The fluorescence spectrum and lifetime measurement is carried out in five wavebands between 333 nm and 694 nm. In a final step, the polarised side-scattering of the particle is measured for 10 ms. The Swisens Poleno Neptune is exactly the same instrument as the Jupiter device, except that it does not have the hardware for the fluorescence and polarization measurements. The Swisens Poleno Mars is a more compact instrument with the same holographic imaging setup but with the measurement located closer to the concentrated particle air nozzle. In principle, this results in a narrower particle position distribution on the raw holographic images without affecting the reconstructed particle images. This model is optimized for monitoring pollen, therefore the detection limit is at a higher particle size than either the Poleno Jupiter or Neptune. Since only pollen is relevant in this measurement campaign, the sensitivity of the particle trigger was set for all Swisens Poleno devices so that small particles were not measured.

Three separate algorithms were applied to the data from the Swisens instruments. The MeteoSwiss algorithm makes use of a two-step classifier, as first developed by Sauvageat et al. (2020), and fully described by Crouzy et al. (2022). In brief: the first step involves filtering out non-biological particles with physically-based criteria, i.e. particle area and solidity, which are both required to fall within the range typical for pollen. Once the pollen particles have been selected, a CNN is applied to classify particles into different taxa. A vision model, largely inspired by the VGG model (Simonyan and Zisserman, 2015) is applied to both the holographic images and features obtained, and then merged into a final, fully-connected layer. The neural network provides a measure of the classification uncertainty in addition to the class. The algorithm applied in this study does not make use of the fluorescence or polarization features measured by the Swisens Poleno Jupiter. From hereafter, the results from the different instrument variants will be noted as follows, Pol-M for the Swisens Poleno Mars, Pol-N for the Swisens Poleno Neptune, and Pol-J for the Swisens Poleno Jupiter. The addition MSw or FMI denotes that the classification algorithm was developed by MeteoSwiss or the Finnish Meteorological Institute (FMI).

Two other classification algorithms were developed by the FMI. The first closely followed the approach proposed by Sauvageat et al. (2020) with the same CNN architecture. The training dataset was built upon pollen samples of species common to Southern Finland. These samples were collected and dried in different countries in 2019 and provided to FMI's Swisens Poleno Jupiter in February 2021. Invalid events were filtered out based on shape and size, eliminating outliers (the same nomenclature is used, e.g. for the Swisens Poleno Mars, the shorthand of Pol M FMI-1 is used). The second version of FMI's algorithm was developed using training datasets from samples collected in Finland in 2021 and provided to FMI's device in late November 2021 in relatively fresh condition. The training procedure of this algorithm used a more sophisticated approach to filtering invalid events, including UMAP dimension reduction and other statistical techniques. Fluorescence measurements were not used by FMI's recognition algorithms in this campaign due to differences in fluorescent excitations between FMI's and the campaign's Swisens Poleno Jupiter devices. The same nomenclature as for the MeteoSwiss algorihms is used, e.g. for the Swisens Poleno Mars, the shorthand of Pol M FMI-2 is used. Recently, the identification of *Alternaria* spores has also been reported (Erbet al, n.d.).

2.3.8. Yamatronics KH-3000

The Yamatronics KH-3000 samples air at a rate of 4.1 L/min (Kawashima et al., 2007). Air flows through an optical system where each particle is hit by scattered light from a 780 nm semiconductor laser. Two signals, forward- and sideward-scattered pulses, are measured and their peak intensities recorded. Differences between the side and forward intensities are a rough indicator of the particle shape and surface roughness (Mishchenko et al., 2000). For this study, a fixed extraction window was used to produce total pollen counts following Kawashima et al., 2017. Temperature effects are removed by automatic control of the laser and while a correction for avoiding any interference from snowfall episodes has been developed, it was not used for this campaign. Instead, similar to some of the other devices, data for periods when rainfall was >2 mm/h were set to zero.

2.4. Statistical analysis

All systems were compared with the mean of all Hirst-type traps that were working at a given time (n = 2–4, mostly 4, see Fig. 1). Hourly data were averaged to 3-hourly or daily values, when at least two thirds of the data (Tummon et al., 2022) were available for that period (i.e. two hours for the 3-hourly data and 16 h for the daily values). The interval of 3 h was selected so as to be able to compare all instruments, since the BAA500 did not provide data at higher temporal resolution for this campaign. For devices that had more than one algorithm (APS, BAA500, Swisens Poleno, Rapid-E, etc.), each algorithm was treated independently as if the results were from a different measurement system.

A different scaling factor (SF) for each system and each pollen taxon as well as total pollen was applied, similarly to Tešendić et al. (2020). In brief, the SF was used to compare automatic systems with manual measurements and is based on the ratio between 95th percentiles from the Hirst and from each automatic system. This ratio was then multiplied by the total seasonal pollen counts of each specific pollen type and for total pollen. The 95th percentile is a value in a given dataset that is greater than the remaining 95 % of values, and its use limits the impact of outliers, which can considerably affect mean values. For those systems where data was not available for the entire campaign, the SF was calculated just for the period they were run. SF = 1 indicates that the pollen concentration measured by the automatic system matches that from the Hirst device exactly. Higher (lower) SF means that the magnitudes given by the automatic systems are lower (higher) than the Hirst.

Total pollen was calculated by summing the concentrations of all pollen taxa counted, which was not necessarily the same for each system (see Table S2).

For each pollen type and system, four statistics were calculated:

- The R^2 (coefficient of determination) is the proportion of the variation in the dependent variable (automatic devices) that can be predicted from the independent variable (Hirst). The slope is a parameter considering the rate of change in concentrations from the automatic system (y) over the change in concentration from the Hirst count (x).
- The Mean Absolute Error, MAE, is the mean absolute value of the individual prediction errors between the value considered as “true”, which here is assumed to be from the Hirst (y_i), and the “predicted” value from the automatic system (y_p). MAE has some advantages, such as that it is robust against outliers, and is simple in concept.
- The Wilcoxon signed-rank test (since the data are non-parametric and paired) was used to test if the data for automatic systems are statistically significantly different from the Hirst measurements.

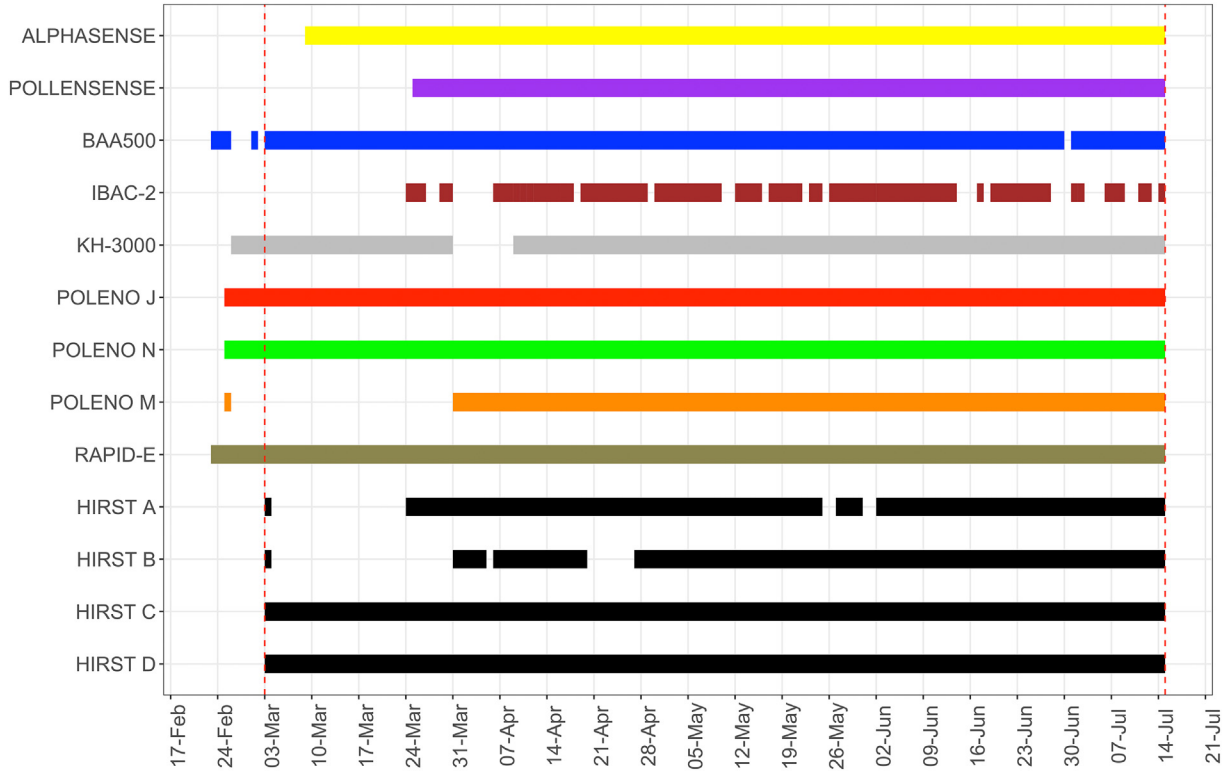

Fig. 1. Data availability for each participating instrument. The beginning of each bar shows the installation date of each device. The Poleno M. (Mars), Hirst A, and Hirst B were replaced due to malfunctioning after an initial measurement period. The vertical red dashed lines show the start and end date of the official campaign (3 March-14 July 2021). Gaps are defined on an hourly basis.

- The Spearman rank coefficient (r), provides an estimate of the correlation between different systems. Because of similarities between some systems, we may expect higher correlations between systems sharing the same algorithms and between devices sharing the same principles, but lower correlations with all others.

Finally, to assess the differences between algorithms applied to the same device, the Friedman test (Friedman, 1940) was performed for those instruments for which three or more results were available (i.e. the Swisens Polenos and the Rapid-E). When $p < 0.05$, a Dunn's post-hoc test (Dunn, 1964) was used, correcting the *p*-value using the Bonferroni method. For the PollenSense, BAA500, and Rapid-E (where $n = 2$), the Wilcoxon signed-rank test was applied instead. Statistical differences in all cases were reported when *p*-values were < 0.05. All data treatment and the analysis were performed in R (R Core Team, 2021), with the packages *Tidyverse* (Wickham et al., 2019), *AeRobiology* (Rojo et al., 2019b), *openair* (Carslaw and Ropkins, 2012) and *lubridate* (Grolemund and Wickham, 2011).

2.5. Meteorological data

Meteorological data for Munich for the campaign were obtained from the German National Meteorological Service (DWD), using the R package *rdwd* (Boessenkool, 2021). Data from the München-City station, located 7.5 km away from the sampling site were acquired, with the following meteorological parameters: air pressure (hPa), air temperature (°C), rainfall (mm), relative humidity (%), sunshine duration (hourly sum, in minutes), wind direction (°) and wind speed (m/s).

2.6. Pollen taxa chosen for this study

In addition to total pollen, several individual pollen taxa were selected for more in-depth analysis. The choice of taxa was a compromise between a) the importance of each pollen type in terms of allergenicity, b) the number of devices capable of distinguishing that particular pollen, c) technical problems (e.g. the main pollen season for *Alnus* and *Corylus* was largely missed since the Hirst data are available only from 3 March 2021 onwards, and second, some devices, such as the APS or Swisens Poleno Mars, did not start functioning until late March due to problems with connectivity or with some of their components), and d) the seasonal abundance as observed in the Hirst data. Four pollen taxa were thus selected: *Betula*, Poaceae, *Fraxinus*, and *Quercus*. Other pollen taxa, such as *Alnus*, *Corylus, Pinus,* Taxaceae/Cupressaceae or Urticaceae, are not discussed further in this paper but results can be visualized in the following online application: *autopollen-interactive.shinyapps.io/022_APP_AUTOPOLLEN*. This application also provides better detail for the discussed pollen taxa for each automatic system in comparison to manual reference counts.

3. Results and discussion

3.1. General aspects regarding the campaign

Overall, the intercomparison campaign demonstrated that several automatic monitoring systems perform well in comparison with the current standard Hirst-type observations. They potentially even overcome some of the issues related to the manual method such as differences between counters (Sikoparija et al., 2017; Oteros et al., 2020), inaccurate sampling volumes related to variability in airflow (Oteros et al., 2017; Triviño et al., 2023, *submitted*), or increased uncertainty at low pollen concentrations (Chappuis et al., 2020; Oteros et al., 2020; Adamov et al., 2021). This campaign also highlighted various aspects about the standardisation of practices for such instrument comparisons, for example, the importance of good site selection, independent operators, and a completely blind comparison of all participating devices. Equally important are several issues related to the analysis, including assessing performance over the whole measurement period to ensure any detection of pollen outside of the main

pollen seasons and the fact that all algorithms should be compared, not just different instruments. Further publications tackling specific aspects of the campaign in more detail are in preparation.

One of the limitations of this study was that the Hirst counts were not completely blinded, i.e. the technicians knew which part of the season they were analysing and this potentially may have influenced the pollen counts since human counters may smooth the start and end of the main pollen season (even if subconsciously) and peaks outside of the season ignored. In a small number of cases we observed pollen peaks with several automatic devices while the Hirst reported none, indicating that they may have been missed in the manual counts. This may have resulted either from the low sampling of the Hirst traps or because of issues with the counting. Another possible error is related to the impaction efficiency of the Hirst-type traps, with differences in flow rates that potentially have an influence on the efficiency of particle impaction on to the adhesive depending on size or even ornamentation (Razmovski et al., 1998). Finally, the use of Hirst-type pollen traps as reference instruments, and the lack of reference measurements more generally (externally calibrated pollen concentrations) is also a limitation, although one that is not possible to overcome at this time. Even so, a number of measures to minimize errors were taken, including, for example, that the pollen counts were performed in the same laboratory, the flow for all traps was corrected with resistance-free flowmeters (Oteros et al., 2017; Triviño et al., 2023, *submitted*), and the clocks checked to ensure optimal performance (Triviño et al., 2023, *submitted*), and the mean of 4 traps was used.

3.2. Data availability and device reliability

For the duration of the campaign most devices showed very good reliability (Table 1, Fig. 1), with data availability ranging from 73.1 % (IBAC-2) to 100 % of the time (Rapid-E, Poleno Jupiter, Poleno Neptune). The high reliability reported here agrees with previous experience with devices such as the BAA500 (Oteros et al., 2020) and the PAA-300, precursor of the Rapid-E (Crouzy et al., 2016). The only gaps in data were due to malfunctions of the device or parts of it (e.g. for the IBAC-2 and Poleno Mars), failures resulting from electrical shortcuts outside the instrument (BAA500, KH-3000), or provoked by overheating of the ventilation system (BAA500). Some instruments, such as the Alphasense, the APS or the IBAC-2, started measurements later because of logistical delays with transport, set-up problems, or in the case of the APS, the need to be connected to the internet to compute particle classifications. Although the Hirst devices are considered robust and are expected to perform continuously outdoors (Beggs et al., 2017), two of the four devices malfunctioned at the beginning of the intercomparison. Hirst A was replaced early in the campaign due to problems with the clock (81.4 % data available), while Hirst B was replaced at a later date because of problems with the pump (72.6 % data available). Hirst C and D worked continuously for the entire campaign.

3.3. Scaling factors

The scaling factors for each system and pollen type are presented in Fig. 2. There is a large spread across devices for all pollen taxa, but the largest differences of up to 20-fold were observed for *Betula*. The systems that fall within the orange dashed vertical lines in Fig. 2 have scaling factors that are within a factor of two of the Hirst average (i.e. the automatic system has values 2 times higher or lower than the Hirst). This is considered reasonable given the uncertainty of the manual counts. There are, however, several instruments that have considerably higher or lower scaling factors, with no discernible pattern across pollen taxa. The differences in scaling factor depend on the pollen type, even between otherwise identical instruments and classification algorithms. Overall, there is no single system that appears to provide a result within a range of factor 2 for all parameters considered (individual pollen taxa and total pollen). The use of a scaling factor for comparison between the automatic systems and the manual baseline should ideally be avoided, even if this method has been used in previous studies (Kawashima et al., 2017; Šaulienė et al., 2019; Tešendić et al., 2020). Given the errors related to the manual counts, scaling against the Hirst may simply increase the error in the automatic system and does not facilitate the comparison between automatic systems. Indeed it may even mask their real capabilities. For example, if one system detected more pollen for one taxon than the Hirst (slope > 1) but we applied a SF, it would reduce the slope of this system, reducing it to a value closer to 1. Rather, more advanced methods (e.g. Lieberherr et al., 2021) should be applied to accurately assess the number counts of automatic systems, even if these have not yet been developed for pollen or other bioaerosol particles.

3.4. Total pollen

In general, larger mean absolute error (MAE) values are observed for total pollen compared to the individual taxa (Fig. 3). It is important to note that most identification algorithms were developed to classify individual pollen taxa and the total pollen shown here is the sum of all trained individual taxa available, which varied from one system to the other (Table S2). Obtaining good results for this category (if the system is able to distinguish well between pollen and other particles) can thus simply be the result of increasing the list of available taxa. This approach can thus only be considered as a rough proxy for real total pollen. Results for the daily averages are considerably better than for the 3-hourly values (Fig. 3 and Table S3). This is to be expected, since the temporal averaging applied to obtain daily values results in less deviation between instruments, either automatic or manual (Crouzy et al., 2016; Adamov et al., 2021). Nevertheless, for the 3-hourly values, 9 out of the 18 systems have R^2 values >0.5. For daily averages, also 9 out of the 18 systems show $R^2 > 0.5$, but with 3 of them with values of $R^2 > 0.75$ (equating to excellent agreement with the manual observations).

The devices that provided only observations of total pollen (KH-3000, Alphasense, IBAC-2) performed relatively poorly. It should be noted, however, that the latter two devices were not initially designed to provide pollen concentrations but rather particle counts or fluorescent particle counts. Furthermore, these devices frequently showed false positives in periods with no pollen. It is possible that this can be attributed to high humidity, fog, or snow events during the months of March and April, even if corrections (when rainfall >2 mm) for this issue were applied. Indeed, for the KH-3000, meteorological conditions are quite important to effectively filter out rainfall events. An alternative explanation for the higher particle counts may be the construction work that was ongoing close by, which may have resulted in localised dust events that potentially may have caused artificial peaks and affected the instruments that measure coarse particulate matter concentrations rather than total pollen (i.e. Alphasense). This phenomenon has also been observed at other sites with other devices (e.g. Šikoparija, 2020). Finally, for the IBAC-2, it is important to mention that the data from the size bin (>1.5 μm) provided is unlikely to be appropriate for just pollen since it also almost certainly includes dust and other small bioaerosols (bacteria, fungal spores, etc.).

3.5. Individual pollen taxa classification

Despite having multiple advantages compared to the Hirst-type traps, the number of false positives identified by the automatic devices both outside and during the main pollen season needs to be reduced. This is particularly important for allergy sufferers, for whom it is important not to issue false alarms. False negatives or more metrics about the systems have not been included in this work, since it is beyond the scope of this article. To fairly compare different algorithms, the same taxa should be included in any confusion matrix used (Tummon et al., 2022), however, this was not possible in this campaign (Table S2). Rather, Spearman's rank coefficient (r) between systems for each pollen type is shown in Table S4. These results indicate that the systems had the highest number of correlations >0.7 for *Betula* (53.3 % of all possible cases), then for *Quercus* (47.5 %), *Fraxinus* (39.7 %) and finally for Poaceae (24.2 %).

3.5.1. Betula

In terms of goodness-of-fit, most systems performed best for *Betula* (Fig. 3), with several devices having $R^2 > 0.5$ (equivalent to a correlation

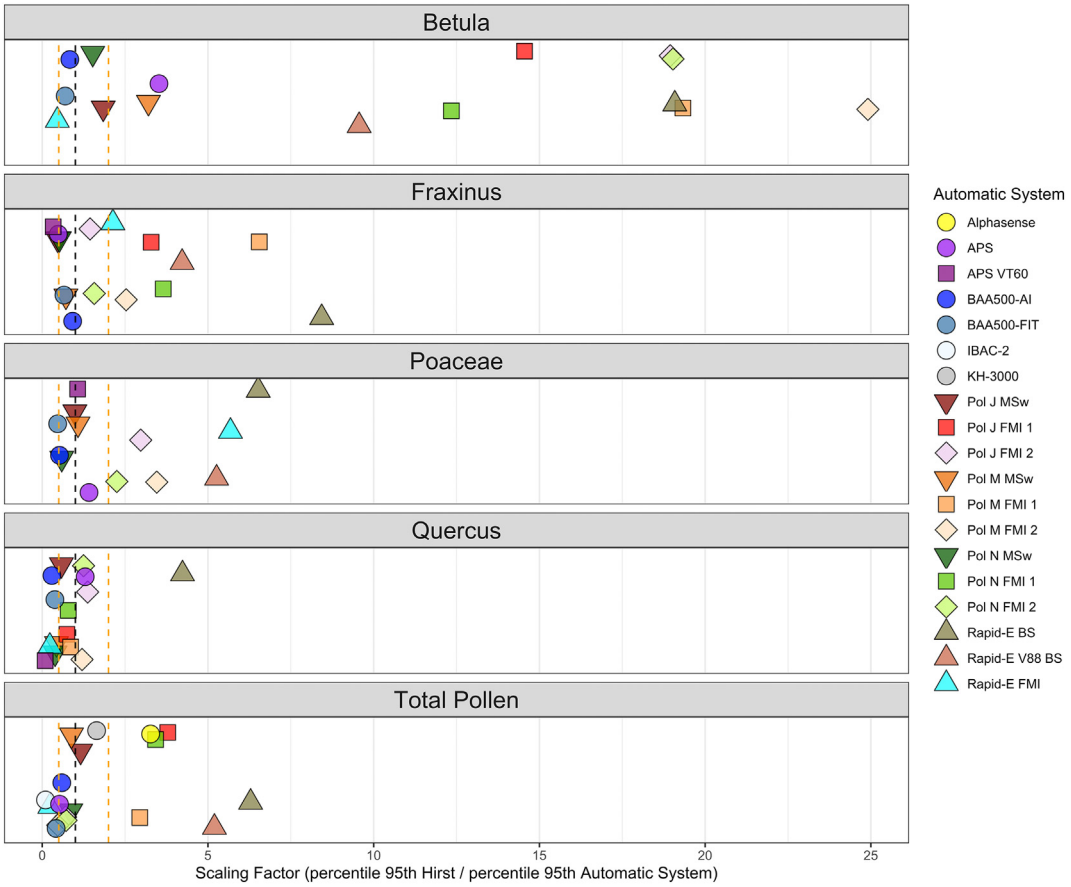

Fig. 2. Scaling Factor (SF) for each system and different pollen taxa/total considered in this study. The black vertical dashed line indicates SF = 1 (no scaling), while the orange vertical dashed lines show the limit between SF = 0.5 (the automatic system has values 2 times higher than the Hirst) and SF = 2 (the automatic system is two times lower than the Hirst).

coefficient of >0.7) and MAE < 20. Overall, the systems that performed best were the BAA500 and Swisens Polenos, with only four systems not reaching R^2 values >0.5 at 3-hourly resolution (the three Rapid-E systems and the APS). Similar performances for the identification of *Betula* have been reported in the past for related systems (Oteros et al., 2015, 2020; Crouzy et al., 2016; Tešendić et al., 2020). Some misclassification issues have been reported by other authors for the Rapid-E systems for the family of Betulaceae (Šaulienė et al., 2019), although in this study this issue was only observed for the Rapid-E FMI algorithm, which showed a slightly lower MAE value (69.06 vs. 70.48) and the same coefficient of determination for the combination *Alnus* + *Corylus* + *Betula* than for *Betula* alone.

Fig. 4a shows the time series for *Betula* for each of the devices capable of distinguishing these pollen taxa. The systems performed well over the main pollen season but some showed false positive classifications (assuming the Hirst results are correct) outside of the main season. The Pol N MSw algorithm shows a peak in *Betula* on 4 March when in fact *Alnus*, *Corylus* and Cupressaceae/Taxaceae are present, the Rapid-E BS a peak on 13 March when Cupressaceae/Taxaceae is present, the BAA500-AI on 25 May when *Quercus* is abundant, the Pol M FMI 1 on 4 June when in fact Poaceae are present, and the Rapid-E FMI on 12 July when Urticaceae are present. Relatively simple methods (e.g Crouzy et al., 2022) exist that can be used to deal with the issue of the identification of false positives but were not applied in any of the algorithms except the Pol MSw algorithms. Future development should take such methods into account and could result in significantly improved performance in terms of incorrect classifications outside of the main pollen season.

3.5.2. *Fraxinus*

The BAA500 algorithms, as well as some of the Swisens Poleno algorithms, showed good scores for *Fraxinus* ($R^2 \approx 0.75$ and MAE < 6 for 3-hourly values), although the scores were lower than for *Betula*. The Rapid-E and APS did not perform as well, neither did the Poleno N FMI 1 and Pol J FMI 1 algorithms. The poorer performance is likely related to false positive classifications outside of the main pollen season, with peaks of >200 pollen grains/m^3 observed for both the Pol J FMI and Pol N FMI algorithms on 4, 11, and 24 March as well as for the Rapid-E BS algorithm on 4 March. On these days, *Alnus*, *Corylus* and Cupressaceae/Taxaceae were present rather than *Fraxinus*. Furthermore, after the main pollen season, false *Fraxinus* positives appeared for the Pol M FMI 1 algorithm on 20 June when *Pinus*, Urticaceae and Poaceae were present, and for both BAA500 algorithms on 5 June when Poaceae was present. The APS reported high numbers of false positives on several days, with peaks >100

Fig. 3. a. Statistical summary of the campaign. Scatter plot showing R^2 (coefficient of determination) vs MAE (Mean Absolute Error) for all systems and pollen taxa considered. The automatic systems are compared to the manual Hirst-type observations for 3-hourly averages. R^2 is a positively-oriented score (higher values show a better agreement with the Hirst), whilst MAE is a negatively-oriented score (lower values indicate better agreement with the Hirst). Note the different x-axis scales. b. Statistical summary of the campaign. Scatter plot showing R^2 (coefficient of determination) vs MAE (Mean Absolute Error) for all systems and pollen taxa considered. The automatic systems are compared to the manual Hirst-type observations for daily averages. R^2 is a positively-oriented score (higher values show a better agreement with the Hirst), whilst MAE is a negatively-oriented score (lower values indicate better agreement with the Hirst). Note the different x-axis scales.

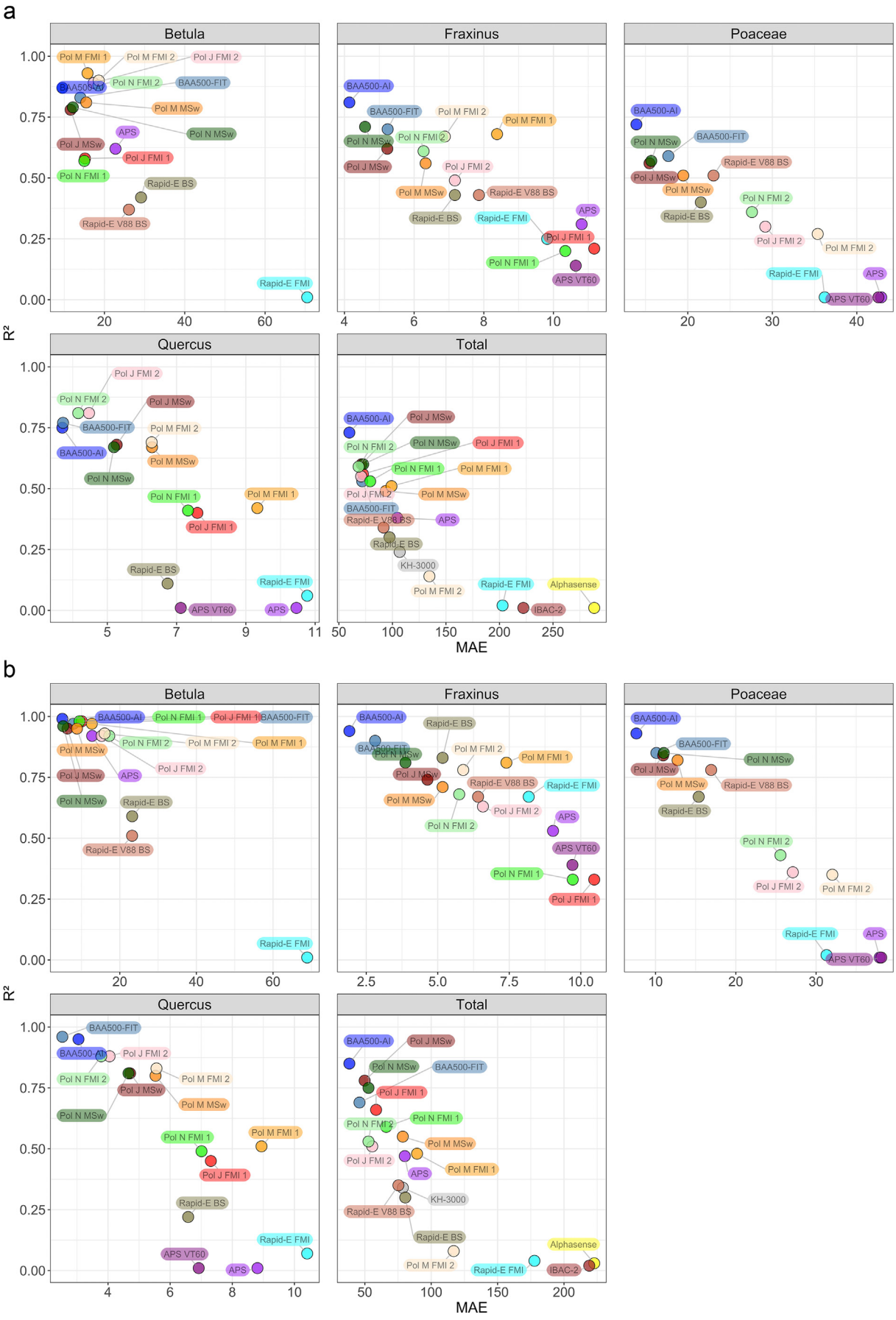
a
Betula
Fraxinus
Poaceae
Quercus
Total
R²
MAE
b
Betula
Fraxinus
Poaceae
Quercus
Total
R²
MAE

pollen grains/m^3 on 10 and 21 May when instead *Quercus* and *Pinus* were airborne, on 17 May when *Fraxinus* was possibly confused with *Quercus*, and on 10 June when it was rather Poaceae and Urticaceae that were present.

3.5.3. Poaceae

In terms of individual taxa, the lowest performance was seen for Poaceae for which none of the systems reached a $R^2 > 0.75$ for 3-hourly data and only 6 for daily resolution. The best scores were achieved by both BAA500 algorithms (AI and FIT) and for the three MeteoSwiss Poleno algorithms (Pol J MSw, Pol N MSw and Pol M MSw). A possible explanation for these lower identification capabilities could be the higher variability in size within the Poaceae family, with a sequence of different species flowering over the pollen season (Frenguelli et al., 2010; Tormo et al., 2011). Other explanations include possible confusion with mist or water droplets, which has been observed previously, or as seen for the PollenSense, the small size of its image library (Jiang et al., 2022). Many of the systems showed days when Poaceae were confused with other pollen types outside of the main pollen season. For example, on 22 and 27 April (when *Betula* and *Fraxinus* were present) and 12 July (Urticaceae) for the APS VT60 algorithm, or 31 March (*Fraxinus* and Cupressaceae/Taxaceae), 8 and 11 April (*Fraxinus*, Cupressaceae/Taxaceae and *Betula*), or 12 July (Urticaceae) for the three MeteoSwiss Poleno algorithms. For the Pol M FMI 2 and Pol N FMI 2 systems, issues were seen on 1 April (*Fraxinus* and Cupressaceae/Taxaceae), 10 April (*Fraxinus*, Cupressaceae/Taxaceae and *Betula*), 25 May (*Pinus* and *Quercus*), as well as on and 29 and 30 May (*Pinus*). For the Rapid-E systems, false positives were detected on 28 April by the Rapid-E V88 (*Fraxinus*) as well as on 4 May (*Betula*), and 25 May (*Pinus* and *Quercus*), and finally the Rapid-E FMI system identified one peak of over 1250 pollen grains/m^3 on 12 July when in fact it was largely Urticaceae that were present in the atmosphere. For the BAA500 systems, both algorithms (FIT and AI) showed small peaks of 40–60 pollen grains/m^3 between 24 March and 26 April before the start of the main pollen season (presence of Cupressaceae/Taxaceae, *Betula*, *Fraxinus* and *Quercus*).

3.5.4. Quercus

The performance for identification of *Quercus* was similar to that for *Fraxinus*, with the best results obtained by both BAA500 systems (FIT and AI) algorithms and the Poleno algorithms (Pol J FMI 2 and Pol N FMI 2), with a higher R^2 for these two Poleno algorithms but lower error (MAE) for the BAA500. The lowest scores were seen for the Rapid-E and PollenSense systems. Nevertheless, all systems identified false events, particularly before the main pollen season. For example, for the APS algorithm on 22 April (presence of *Betula*, *Fraxinus* and Cupressaceae/Taxaceae) and 12 June (Poaceae and Urticaceae) or for the APS VT60 on 30 March (presence of *Fraxinus* and Cupressaceae/Taxaceae), 5 April (*Fraxinus*), and 12 June (>200 pollen grains/m^3, presence of Poaceae and Urticaceae). The BAA500 had false peaks of around 40 pollen grains/m^3 on 31 March – 1

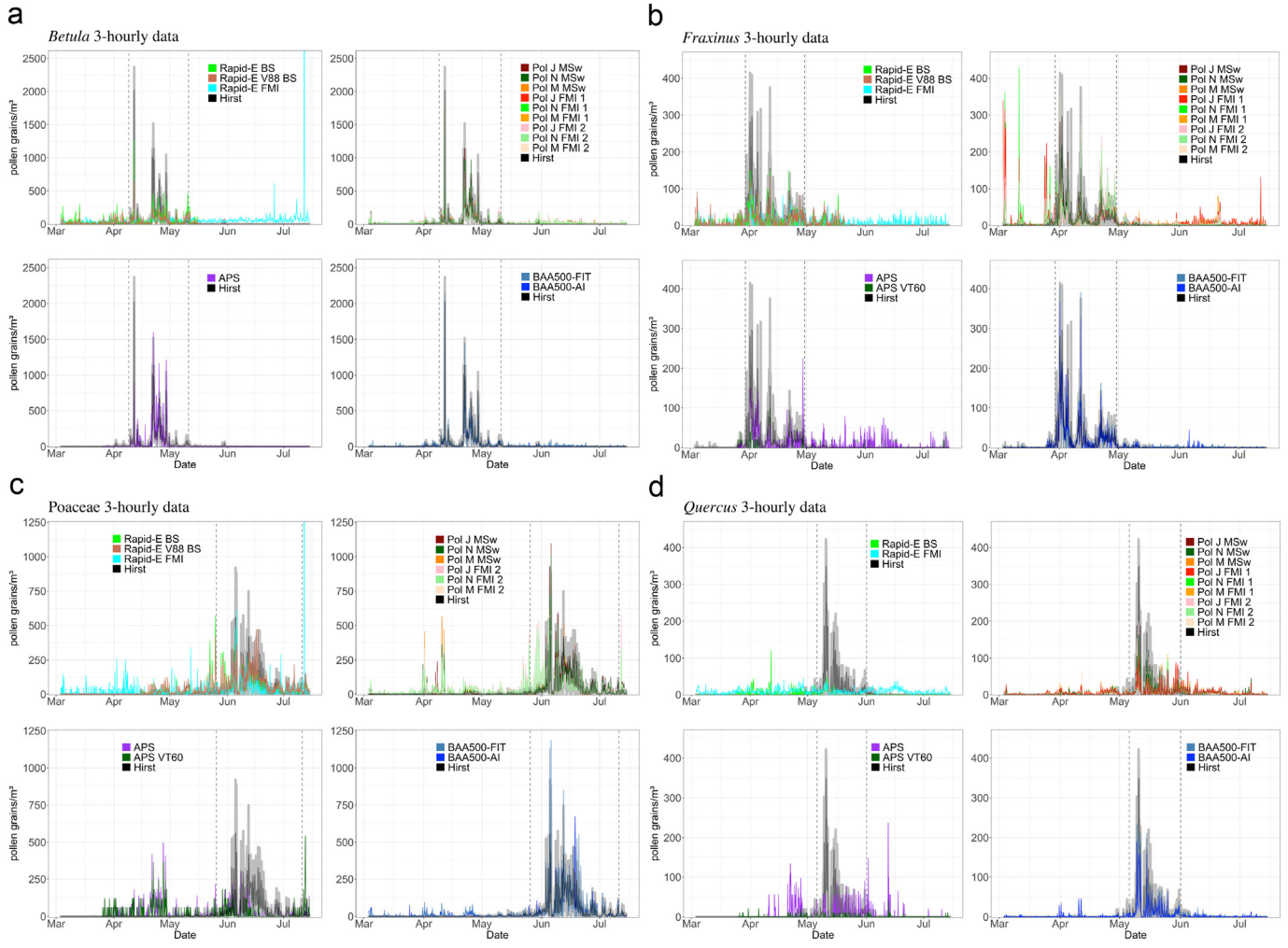

Fig. 4. Time series for systems that report individual pollen classifications. Data for a) *Betula*, b) *Fraxinus*, c) Poaceae and d) *Quercus*. The black timeseries represents the mean of all Hirst devices working at each particular time (n = 2–4) while the grey shading provides the range across all Hirst-type traps. The vertical black dashed lines represent the start and end date of the main pollen season (calculated using the 95 % method). Note the different y-axis scales. Further figures for other pollen taxa (including total pollen) and other systems can be visualized through the interactive graphs available at: *autopollen-interactive.shinyapps.io/022_APP_AUTOPOLLEN*.

April (Cupressaceae/Taxaceae and *Fraxinus*), 60 pollen grains/m^3 on 10–11 April (Cupressaceae/Taxaceae, *Fraxinus* and *Betula*), and < 30 during much of June (Poaceae, Urticaceae and *Pinus*). For all Swisens Poleno systems, some peaks with concentrations around 20 pollen grains/m^3 were also observed in June and a peak of >45 pollen grains/m^3 on 6 July (Urticaceae and Poaceae). Furthermore, prior to the season, issues were also identified on 11 April (Cupressaceae/Taxaceae, *Fraxinus* and *Betula*). Finally, the Rapid-E falsely identified *Quercus* over much of the period, with two particularly large peaks for the Rapid-E BS occurring on 2 and 11 April (when Cupressaceae/Taxaceae, *Fraxinus* and *Betula* were present).

3.6. Differences between algorithms applied to the same device

Table 2 shows the statistical differences calculated for each of the algorithms applied to each of the instruments for the different pollen taxa presented in this study. Fig. 5 presents how the results for each system are distributed in terms of R^2 and MAE. As already mentioned, bigger differences between all systems were seen at the 3-hourly resolution than for the daily averages.

3.6.1. PollenSense

For the PollenSense instrument, statistically significant differences were seen between the APS and APS VT60 algorithms for *Fraxinus*, Poaceae, and *Quercus*, while *Betula* and Total Pollen were not evaluated with the APS VT60 algorithm. Both systems showed similar values regarding the quality of results, although the APS algorithm performed slightly better (Fig. 3), and further algorithm training for European taxa would help to improve performance, particularly for Poaceae and *Quercus*.

3.6.2. BAA500

Statistically significant differences ($p < 0.05$) were found for all pollen types between the BAA500-FIT and BAA500-AI algorithms, with the latter algorithm performing better in all cases except for *Quercus*. These differences can be attributed to the different structure of the algorithms, the latter being considerably more complex, stable and less sensitive to small datasets (Tharwat et al., 2017).

3.6.3. Swisens Poleno

For the Swisens Poleno, most differences between the systems were observed for *Fraxinus* (9 out of 9 cases for 3-hourly and 8 for daily values) and the fewest for total pollen (5 out of 9 cases for 3-hourly values and none for the daily averages). In comparison with the Hirst observations (Fig. 3), the algorithms developed by MeteoSwiss ranked higher for *Fraxinus* and Poaceae, whilst the FMI (in particular FMI 2) algorithms performed better for *Quercus*. For *Betula* and total pollen, the algorithms performed similarly, with the MeteoSwiss systems having lower R^2 values but also lower MAE for *Betula,* while the contrary was seen for total pollen. Overall, the second version of the FMI algorithm (FMI-2) performed better than the first version of the algorithm (FMI-1) trained using dry pollen and less sophisticated data cleaning techniques.

3.6.4. Plair rapid-E

The Rapid-E algorithms from the BioSense Institute (Rapid-E BS and Rapid-E V88 BS) were different from that of the FMI (Rapid-*E*-FMI) for *Betula*, Poaceae, *Quercus*, and total pollen.For *Fraxinus* we only find differences for the Rapid-E BS compared to the FMI algorithm. The fluorescence threshold used to filter the *Betula* data in the Rapid-E FMI algorithm is potentially too low, allowing too many events to pass through and many of the resulting concentrations being too high (i.e. the true signal being flooded by other particles). In contrast, having a training dataset collected from four different devices for the BS algorithm may have resulted in an algorithm trained to identify differences between devices rather than between pollen taxa if the fluorescent signals are different for the same species measured by different Rapid-E devices. The two algorithms from the Biosense Institute were similar only for total pollen, but in comparison with the Hirst observations better results were obtained for the Rapid-E BS for *Fraxinus* and for Rapid-E V88 BS for total pollen. For the FMI algorithm, pollen counts were multiplied by a value of 2, which is an efficiency coefficient roughly estimated from previous experience (Šaulienė et al., 2019).

4. Conclusions

An international intercomparison of automatic bioaerosol monitors was organised within the framework of the EUMETNET AutoPollen Programme and the ADOPT COST Action. The campaign took place in Munich,

Table 2
3-hourly and daily statistical differences between systems. ns, *, ** and *** represent *p*-values of non-significant (> 0.05), ≤ 0.05, ≤ 0.01, and ≤ 0.001, respectively.

		Betula				*Fraxinus*				Poaceae				*Quercus*				Total Pollen			
		3-hourly data		Daily data		3-hourly data		Daily data		3-hourly data		Daily data		3-hourly data		Daily data		3-hourly data		Daily data	
System 1	System 2	n	p.adj. signif	n	p.adj. signif	n	p.adj. signif	n	p.adj. signif	n	p.adj. signif	n	p.adj. signif	n	p.adj. signif	n	p.adj. signif	n	p.adj. signif	n	p.adj. signif
APS	APS VT60	–	–	–	–	891	***	111	***	891	***	111	***	891	***	111	***	–	–	–	–
BAA500-AI	BAA500-FIT	1035	***	129	***	1035	***	129	***	1035	***	129	***	1035	***	129	***	1035	***	129	***
Pol J FMI 1	Pol J FMI 2	820	ns	101	ns	820	***	101	***	–	–	–	–	820	***	101	**	820	***	101	ns
Pol J FMI 1	Pol J MSw	820	***	101	***	820	***	101	*	–	–	–	–	820	***	101	ns	820	ns	101	ns
Pol J FMI 2	Pol J MSw	820	***	101	***	820	***	101	ns	820	***	101	ns	820	ns	101	ns	820	***	101	ns
Pol M FMI 1	Pol M FMI 2	820	*	101	ns	820	***	101	***	–	–	–	–	820	***	101	**	820	ns	101	ns
Pol M FMI 1	Pol M MSw	820	***	101	***	820	***	101	***	–	–	–	–	820	***	101	**	820	*	101	ns
Pol M FMI 2	Pol M MSw	820	***	101	***	820	***	101	***	820	***	101	ns	820	ns	101	ns	820	ns	101	ns
Pol N FMI 1	Pol N FMI 2	820	*	101	ns	820	***	101	**	–	–	–	–	820	***	101	**	820	***	101	ns
Pol N FMI 1	Pol N MSw	820	***	101	***	820	***	101	ns	–	–	–	–	820	***	101	*	820	ns	101	ns
Pol N FMI 2	Pol N MSw	820	***	101	***	820	***	101	**	820	***	101	ns	820	ns	101	ns	820	***	101	ns
Rapid-E BS	Rapid-E FMI	1068	***	134	***	1068	***	133	**	1068	ns	134	ns	1068	***	134	***	1068	***	134	***
Rapid-E BS	Rapid-E V88 BS	1068	***	134	***	1068	***	133	***	1068	***	134	***	–	–	–	–	1068	ns	134	ns
Rapid-E FMI	Rapid-E V88 BS	1068	***	134	***	1068	ns	133	ns	1068	***	134	ns	–	–	–	–	1068	***	134	***

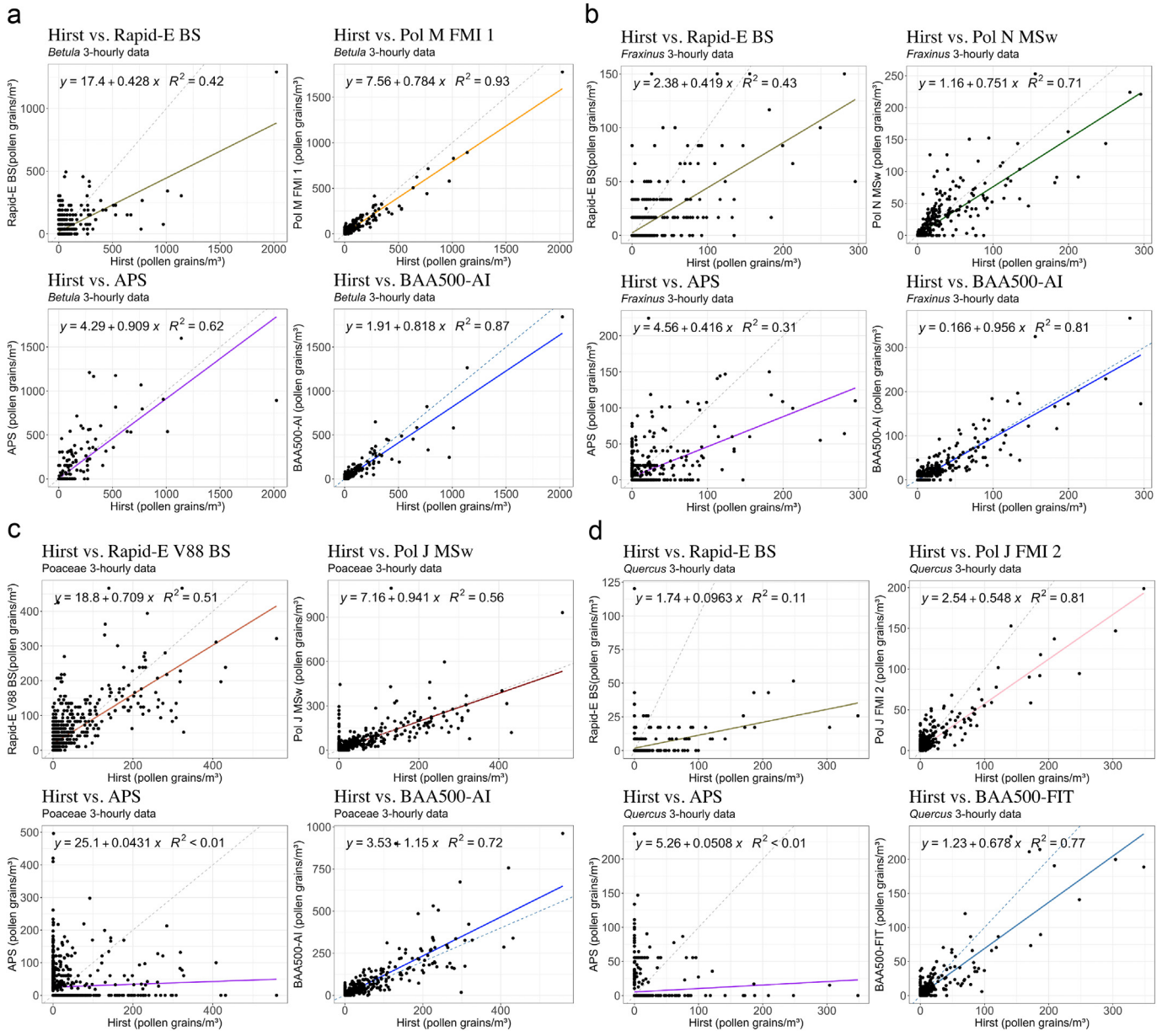

Fig. 5. 3-hourly scatter plots for systems that report individual pollen classifications. The best performing algorithm for each instrument and pollen taxa is shown for a) *Betula*, b) *Fraxinus*, c) Poaceae and d) *Quercus* (the selection was based on a compromise of the best R^2 and slope values). The dashed grey line represents a perfect fit with the Hirst data (slope = 1). Further figures for other pollen taxa (including total pollen) and other systems can be visualized through the interactive graphs available at: *autopollen-interactive.shinyapps.io/022_APP_AUTOPOLLEN*.

Germany, from 3 March-14 July 2021 with 14 participating real-time instruments run in parallel with up to 4 manual Hirst-type traps. Data availability was in general higher than 99 % thus indicating good reliability of the automatic devices. Comparisons with the reference observations (the mean of 4 Hirst traps) in terms of a selection of individual pollen taxa as well as total pollen showed that certain automatic systems (instrument plus identification algorithm) are already well suited for continuous real-time pollen monitoring. In general, results for daily averages agreed better with the baseline of manual observations than for the 3-hourly observations (likely because of the larger variability of the Hirst method at high time resolutions (Adamov et al., 2021)), with the same being true for individual pollen taxa compared to total pollen. Of the four individual pollen taxa considered, the systems capable of distinguishing them provided the best results for *Betula*, *Fraxinus*, *Quercus*, and then for Poaceae, respectively. Several systems showed periods with false positives outside of the main pollen season. Furthermore, different algorithms applied to the same device provided different results, indicating that the entire system (device + algorithm) is important for a good classification. Instruments that were only able to identify total pollen had some issues with interferences, largely due to meteorological conditions, dust events or possible inclusion of other bioaerosols, and did not reach the same data quality levels.

Overall, the results show that several automatic systems delivered results in good agreement with manual Hirst-type observations, but other instruments are far from being operative with the required accuracy. The new systems have the potential to perform even better since they do not suffer from many of the limitations of Hirst-type pollen traps, although there is certainly room for improvement. One key issue in particular is the availability of reference measurements. Until a calibration standard for airborne pollen is developed, the drawback of comparing automatic instruments with the Hirst-type trap, which itself is subject to a number of errors, cannot be circumvented. This again highlights the disadvantage of using a scaling factor to adjust the results of an automatic device to those of the Hirst-type

trap: this adjusts an instrument to replicate the manual data which might in fact not be correct in terms of the real airborne number concentrations.

Our intercomparison evaluates the state of the art in pollen monitoring, identifies specific strengths and possible improvements, encouraging further development to ensure continuous progress for the community and users.

CRediT authorship contribution statement

José M. Maya-Manzano: Data curation, Formal analysis, Investigation, Methodology, Project administration, Software, Validation, Visualization, Writing – original draft, Writing – review & editing. **Fiona Tummon:** Conceptualization, Formal analysis, Investigation, Methodology, Project administration, Resources, Supervision, Visualization, Writing – original draft, Writing – review & editing. **Reto Abt:** Investigation, Resources, Writing – review & editing. **Nathan Allan:** Formal analysis, Investigation, Writing – review & editing. **Landon Bunderson:** Formal analysis, Investigation, Writing – review & editing. **Bernard Clot:** Conceptualization, Formal analysis, Investigation, Methodology, Project administration, Resources, Supervision, Visualization, Writing – original draft, Writing – review & editing. **Benoît Crouzy:** Formal analysis, Investigation, Resources, Writing – review & editing. **Gintautas Daunys:** Investigation, Writing – review & editing. **Sophie Erb:** Formal analysis, Investigation, Writing – review & editing. **Mónica Gonzalez-Alonso:** Formal analysis, Investigation, Writing – review & editing. **Elias Graf:** Investigation, Resources, Writing – review & editing. **Łukasz Grewling:** Formal analysis, Investigation, Validation, Writing – review & editing. **Jörg Haus:** Formal analysis, Investigation, Writing – review & editing. **Evgeny Kadantsev:** Formal analysis, Investigation, Writing – review & editing. **Shigeto Kawashima:** Formal analysis, Investigation, Writing – review & editing. **Moises Martinez-Bracero:** Formal analysis, Investigation, Resources, Writing – review & editing. **Predrag Matavulj:** Formal analysis, Investigation, Writing – review & editing. **Sophie Mills:** Formal analysis, Investigation, Resources, Writing – review & editing. **Erny Niederberger:** Investigation, Resources, Writing – review & editing. **Gian Lieberherr:** Formal analysis, Investigation, Resources, Writing – review & editing. **Richard W. Lucas:** Formal analysis, Investigation, Writing – review & editing. **David J. O'Connor:** Formal analysis, Investigation, Resources, Writing – review & editing. **Jose Oteros:** Formal analysis, Investigation, Writing – review & editing. **Julia Palamarchuk:** Formal analysis, Investigation, Writing – review & editing. **Francis D. Pope:** Formal analysis, Investigation, Resources, Writing – review & editing. **Jesus Rojo:** Investigation, Writing – review & editing. **Ingrida Šaulienė:** Investigation, Writing – review & editing. **Stefan Schäfer:** Formal analysis, Investigation, Writing – review & editing. **Carsten B. Schmidt-Weber:** Formal analysis, Investigation, Resources, Writing – review & editing. **Martin Schnitzler:** Investigation, Writing – review & editing. **Branko Šikoparija:** Formal analysis, Investigation, Supervision, Writing – review & editing. **Carsten A. Skjøth:** Investigation, Writing – review & editing. **Mikhail Sofiev:** Formal analysis, Investigation, Methodology, Supervision, Writing – review & editing. **Tom Stemmler:** Formal analysis, Investigation, Writing – review & editing. **Marina Triviño:** Investigation, Validation, Writing – review & editing. **Yanick Zeder:** Investigation, Writing – review & editing. **Jeroen Buters:** Conceptualization, Formal analysis, Investigation, Methodology, Project administration, Resources, Supervision, Validation, Visualization, Writing – original draft, Writing – review & editing.

Data availability

Data will be made available on request.

Declaration of Competing Interest

The authors declare the following financial interests/personal relationships which may be considered as potential competing interests:

Jeroen Buters, Jose *M. Maya* Manzano, Carsten B. Schmidt-Weber and Marina Triviño report financial support, administrative support, equipment, drugs, or supplies, and travel were provided by Bayerisches Landesamt für Gesundheit und Lebensmittelsicherheit (LGL) and EUMETNET.

Carsten Skjoth reports financial support, administrative support, article publishing charges, equipment, drugs, or supplies, and travel were provided by COST Action CA18226 ADOPT – *New approaches in detection of pathogens and aeroallergens*.

Bernard Clot and Fiona Tummon report financial support, administrative support, article publishing charges, equipment, drugs, or supplies, and travel were provided by European Meteorological Society and the EUMETNET AutoPollen Programme.

Branko Sikoparija and Predrag Matavulj report financial support, administrative support, article publishing charges, equipment, drugs, or supplies, and travel were provided by BREATHE project from the Science Fund of the Republic of Serbia PROMIS program, under grant agreement no. 6039613 and by the Ministry of Education, Science and Technological Development of the Republic of Serbia (grant agreement number 451–03-68/2022–14/200358).

Evgeny Kadantsev and Julia Palamarchuk report financial support, administrative support, article publishing charges, equipment, drugs, or supplies, and travel were provided by Academy of Finland PS4A (grant 318,194).

Mikhail Sofiev reports financial support, administrative support, article publishing charges, equipment, drugs, or supplies, and travel were provided by Academy of Finland project ALL-Impress (grant 329,215).

Mikhail Sofiev reports financial support, administrative support, article publishing charges, equipment, drugs, or supplies, and travel were provided by European Social Fund (project no. 09.3.3-LMT-K-712-01-0066) and Research Council of Lithuania (LMTLT).

Nathan Allan, Landon Bunderson, Richard W. Lucas (Pollen science TM), Jorg Haus, Stefan Schaefer, Martin Schnitzler and Tom Stemmler (Helmut Hund Wetzlar), Reto Abt, Elias Graf, Erny Niederberger and Yanick Zeder (Swisens AG) report a relationship with Pollen science TM, Helmut Hund Wetzlar and Swisens AG respectively, that includes: board membership, employment, and travel reimbursement. The investigations were carried out in compliance with good scientific practices and the support provided by these companies in terms of instrumentation had no effect on the results presented.

Acknowledgements

This article contributes to the EUMETNET AutoPollen Programme, which is developing a prototype European automatic pollen monitoring network. The intercomparison campaign was funded by EUMETNET AutoPollen Programme of which the Bayerisches Landesamt für Gesundheit und Lebensmittelsicherheit (LGL) took part. We also thank financial support from the COST Action CA18226 ADOPT – *New approaches in detection of pathogens and aeroallergens*. We thank the ZAUM team who assisted in the organization and preparation for this campaign: Cordula Ebner von Eschenbach, Gudrun Pusch and Christine Weil; the MeteoSwiss team that assisted in the campaign: Nina Burgdorfer and Sophie Erb; as well as the Helmholtz Zentrum München for hosting the campaign, and the team who assist us during it: Daphne Kolland, George Matuscheck, Benjamin Schnautz and Andreas Westenkirchner. Our special acknowledgement goes to the manual pollen analysts: Łukasz Kostecki and Agata Szymanska. For the IT support we thank Robert Gebauer (external IT specialist), Gisela Nagy and Anton Pointner (Helmholtz Zentrum München). We would like also to thank all the companies or universities kindly providing their devices to participate in this campaign; CRNS Sextant (Dominique Filipi), Droplet Measurement technologies (Darrel Baumgardner, Dagen Hughes, Tobias Könemann, Uwe Michalak), Dublin City University (David O'Connor), Helmut Hund Wetzlar (Jörg Haus, Stefan Schäfer, Martin Schnitzler, Tom Stemmler), MeteoSwiss (Bernard Clot, Benoit Crouzy, Sophie Erb, Gian Lieberherr, Fiona Tummon), PollenSense (Nathan Allan, Landon Bunderson, Kevn Lambson, Richard Lucas), Šiauliai Academy, Vilnius University (Gintautas Daunys, Ingrida Šauliene), Swisens (Reto Abt, Elias Graf, Erny Niederberger, Yannick Zeder), University of Graz (Nam Cao), University of Kyoto (Shigeto Kawashima), University of Birmingham (Sophie Mills, Francis Pope), ZAUM, Technical University Munich (Jeroen

Buters, Jose M. Maya-Manzano, Carsten Schmidt-Weber, Marina Triviño). Branko Sikoparija and Predrag Matavulj were partly funded by the BREATHE project from the Science Fund of the Republic of Serbia PROMIS program, under grant agreement no. 6039613. Evgeny Kadantsev and Julia Palamarchuk have been supported by the Academy of Finland projects PS4A (grant 318194), Mikhail Sofiev was supported by Academy of Finland project ALL-Impress (grant 329215) and by the European Social Fund (project no. 09.3.3-LMT-K-712-01-0066) under grant agreement with the Research Council of Lithuania (LMTLT).

Appendix A. Supplementary data

Supplementary data to this article can be found online at https://doi.org/10.1016/j.scitotenv.2022.161220.

References

Adamov, S., Lemonis, N., Clot, B., Crouzy, B., Gehrig, R., Graber, M.J., Sallin, C., Tummon, F., 2021. On the measurement uncertainty of hirst-type volumetric pollen and spore samplers. Aerobiologia https://doi.org/10.1007/s10453-021-09724-5.

Anderegg, W.R.L., Abatzoglou, J.T., Anderegg, L.D.L., Bielory, L., Kinney, P.L., Ziska, L., 2021. Anthropogenic climate change is worsening North American pollen seasons. Proc. Natl. Acad. Sci. 118 (7), e2013284118.

Bannister, T., Ebert, E.E., Williams, T., Douglas, P., Wain, P., Carroll, M., Silver, J., Newbigin, E., Lampugnani, E.R., Hughes, N., Looker, C., Mulvenna, V., Csutoros, D., Jones, P.J., Davies, J.M., Suphioglu, C., Beggs, P.J., Emmerson, K.M., Huete, A., Nguyen, H., 2021. A pilot forecasting system for epidemic thunderstorm asthma in southeastern Australia. Bull. Am. Meteorol. Soc. 102 (2), E399–E420.

Beggs, P.J., Šikoparija, B., Smith, M., 2017. Aerobiology in the International Journal of Biometeorology, 1957–2017. Int. J. Biometeorol. 61, 51–58.

Boessenkool, B., 2021. rdwd: Select and Download Climate Data from "DWD" (German Weather Service). R package version 1.5.0. https://cran.r-project.org/package=rdwd.

Bousquet, J., Khaltaev, N., Cruz, A.A., Denburg, J., Fokkens, W.J., Togias, A., Zuberbier, T., Baena-Cagnani, C.E., Canonica, G.W., van Weel, C., Agache, I., Aït-Khaled, N., Bachert, C., Blaiss, M.S., Bonini, S., Boulet, L.P., Bousquet, P.J., Camargos, P., Carlsen, K.H., Chen, Y., Custovic, A., Dahl, R., Demoly, P., Douagui, H., Durham, S.R., van Wijk, R.G., Kalayci, O., Kaliner, M.A., Kim, Y.Y., Kowalski, M.L., Kuna, P., Le, L.T.T., Lemiere, C., Li, J., Lockey, R.F., Mavale-Manuel, S., Meltzer, E.O., Mohammad, Y., Mullol, J., Naclerio, R., O'Hehir, R.E., Ohta, K., Ouedraogo, S., Palkonen, S., Papadopoulos, N., Passalacqua, G., Pawankar, R., Popov, T.A., Rabe, K.F., Rosado-Pinto, J., Scadding, G.K., Simons, F.E.R., Toskala, E., Valovirta, E., van Cauwenberge, P., Wang, D.Y., Wickman, M., Yawn, B.P., Yorgancioglu, A., Yusuf, O.M., Zar, H., Annesi-Maesano, I., Bateman, E.D., Kheder, A.ben, Boakye, D.A., Bouchard, J., Burney, P., Busse, W.W., Chan-Yeung, M., Chavannes, N.H., Chuchalin, A., Dolen, W.K., Emuzyte, R., Grouse, L., Humbert, M., Jackson, C., Johnston, S.L., Keith, P.K., Kemp, J.P., Klossek, J.M., Larenas-Linnemann, D., Lipworth, B., Malo, J.L., Marshall, G.D., Naspitz, C., Nekam, K., Niggemann, B., Nizankowska-Mogilnicka, E., Okamoto, Y., Orru, M.P., Potter, P., Price, D., Stoloff, S.W., Vandenplas, O., Viegi, G., Williams, D., 2008. Allergic Rhinitis and its Impact on Asthma (ARIA) 2008 update (in collaboration with the World Health Organization, GA2LEN and AllerGen). Allergy: Eur. J. Allergy Clin. Immunol. 63 (Suppl.86), 8–160.

Buters, J.T.M., Antunes, C., Galveias, A., Bergmann, K.C., Thibaudon, M., Galán, C., Schmidt-Weber, C., Otros, J., 2018. Pollen and spore monitoring in the world. Clin.Transl.Allergy 8 (9).

Buters, J., Clot, B., Galan, C., Gehrig, R., Gilge, S., Hentges, F., O'Connor, D., Sikoparija, B., Skjoth, C., Tummon, F., Adams-Groom, B., Antunes, C.M., Bruffaerts, N., Çelenk, S., Crouzy, B., Guillaud, G., Hajkova, L., Kofol Seliger, A., Oliver, G., Ribeiro, H., Rodinkova, V., Saarto, A., Sauliene, I., Sozinova, O., Stjepanovic, B., 2022. Automatic pollen and fungal spore detectors: an overview. Aerobiologia https://doi.org/10.1007/s10453-022-09750-x.

Carslaw, D.C., Ropkins, K., 2012. Openair — an R package for air quality data analysis. Environ. Model Softw. 27–28, 52–61.

Chappuis, C., Tummon, F., Clot, B., Konzelmann, T., Calpini, B., Crouzy, B., 2020. Automatic pollen monitoring: first insights from hourly data. Aerobiologia 36, 159–170.

Clot, B., Gilge, S., Hajkova, L., Magyar, D., Scheifinger, H., Sofiev, M., Bütler, F., Tummon, F., 2020. The EUMETNET AutoPollen programme: establishing a prototype automatic pollen monitoring network in Europe. Aerobiologia 1–9. https://doi.org/10.1007/s10453-020-09666-4.

Crilley, L.R., Shaw, M., Pound, R., Kramer, L.J., Price, R., Young, S., Lewis, A.C., Pope, F.D., 2018. Evaluation of a low-cost optical particle counter (Alphasense OPC-N2) for ambient air monitoring. Atmos.Meas.Tech. 11, 709–720.

Crouzy, B., Stella, M., Konzelmann, T., Calpini, B., Clot, B., 2016. All-optical automatic pollen identification: towards an operational system. Atmos. Environ. 140, 202–212.

Crouzy, B., Lieberherr, G., Tummon, F., Clot, B., 2022. False positives: handling them operationally for automatic pollen monitoring. Aerobiologia 38, 429–442. https://doi.org/10.1007/s10453-022-09757-4.

Daunys, G., Šukiene, L., Vaitkevichius, L., Valiulis, G., Sofiev, M., Šauliene, I., 2021. Clustering approach for the analysis of the fluorescent bioaerosol collected by an automatic detector. PLOS ONE 16 (3), e0247284. https://doi.org/10.1371/journal.pone.0247284.

DeFreez, R., 2009. LIF bio-aerosol threat triggers: then and now. Optically Based Biological and Chemical Detection for Defence V 7484, 74840H https://doi.org/10.1117/12.835088.

Dunn, O.J., 1964. Multiple comparisons using rank sums. Technometrics 6, 241–252.

Erbet al., n.d.Erb, S., Berne, A., Burgdorfer, N., Clot, B., Graber, M.J., Lieberherr, G., Sallin, C., Tummon, F., Crouzy, B., Short communication: automatic real-time monitoring of fungal spores: the case of Alternaria spp. doi:10.1101/2022.08.03.500168.n.d.

Flir IBAC-2, 2022. Teledyne FLIR [WWW Document]. URL (accessed 3.4.22) https://www.flir.de/products/ibac-2/.

Frenguelli, G., Passalacqua, G., Bonini, S., Fiocchi, A., Incorvaia, C., Marcucci, F., Tedeschini, E., Canonica, G.W., Frati, F., 2010. Bridging allergologic and botanical knowledge in seasonal allergy: a role for phenology. Ann. Allergy Asthma Immunol. 105, 223–227.

Friedman, M., 1940. A comparison of alternative tests of significance for the problem of m rankings. Ann.Math.Stat. 11 (1).. https://www.jstor.org/stable/2235971#metadata_info_tab_contents.

Galán, C., Domínguez-Vilches, E., 1997. The capture media in aerobiological sampling. Aerobiologia 13, 155–160.

Galán, C., Smith, M., Thibaudon, M., Frenguelli, G., Oteros, J., Gehrig, R., Berger, U., Clot, B., Brandao, R., EAS QC Working Group, 2014. Pollen monitoring: minimum requirements and reproducibility of analysis. Aerobiologia 30, 385–395. https://doi.org/10.1007/s10453-014-9335-5.

Glick, S., Gehrig, R., Eeftens, M., 2021. Multi-decade changes in pollen season onset, duration, and intensity: a concern for public health? Sci. Total Environ. 781, 146382.

González-Alonso, M., Boldeanu, M., Koritnik, T., Gonçalves, J., Belzner, L., Stemmler, T., Gebauer, R., Grewling, Ł., Tummon, F., Maya-Manzano, J.M., Ariño, A.H., Schmidt-Weber, C., Buters, J., 2022. Alternaria spore exposure in Bavaria, Germany, measured using artificial intelligence algorithms in a network of BAA500 automatic pollen monitors. Sci. Total Environ. 160180.

Grinnellet al., 1961Grinnell, SW., Perkins, WA., Vaughan, LM., 1961. Sampling apparatus and method. Patent no. 2, 973, 642.

Grolemund, G., Wickham, H., 2011. Dates and times made easy with lubridate. J. Stat. Softw. 40, 1–25.

Healy, D.A., Huffman, J.A., O'Connor, D., Pöhlker, C., Pöschl, U., Sodeau, J., 2014. Ambient measurements of biological aerosol particles near Killarney, Ireland: a comparison between real-time fluorescence and microscopy techniques. Atmos. Chem. Phys. 14, 8055–8069.

Hirst, J., 1952. An automatic volumetric spore trap. Ann.Appl.Biol. 39, 257–265.

Huffman, J.A., Perring, A.E., Savage, N.J., Clot, B., Crouzy, B., Tummon, F., Shoshanim, O., Damit, B., Schneider, J., Sivaprakasam, V., Zawadowicz, M.A., Crawford, I., Gallagher, M., Topping, D., Doughty, D.C., Hill, S.C., Pan, Y., 2020. Real-time sensing of bioaerosols: review and current perspectives. Aerosol Sci. Technol. 54 (5), 465–495.

Hughes, D.D., Mampage, C.B.A., Jones, L.M., Liu, Z., Stone, E.A., 2020. Characterization of atmospheric pollen fragments during springtime thunderstorms. Environ.Sci.Technol.Lett. 7, 409–414.

Isard, S.A., Barnes, C.W., Hambleton, S., Ariatti, A., Russo, J.M., Tenuta, A., Gay, D.A., Szabo, L.J., 2011. Predicting soybean rust incursions into the North American continental interior using crop monitoring, spore trapping, and aerobiological modeling. Plant Dis. 95 (11), 1327–1485. https://doi.org/10.1094/PDIS-01-11-0034 95, 1346-1357.

Jiang, C., Wang, W., Du, L., Huang, G., McConaghy, C., Fineman, S., Liu, Y., 2022. Field evaluation of an automated pollen sensor. Int. J. Environ. Res. Public Health 19 (11), 6444.

Jonsson, P., Kullander, F., 2014. Bioaerosol detection with fluorescence spectroscopy. In: Jonsson, P., Olofsson, G., Tjärnhage, T. (Eds.), Bioaerosol Detection Technologies. Integrated Analytical Systems. Springer, New York, NY, pp. 111–141 https://doi.org/10.1007/978-1-4419-5582-1_7.

Kawashima, S., Clot, B., Fujita, T., Takahashi, Y., Nakamura, K., 2007. An algorithm and a device for counting airborne pollen automatically using laser optics. Atmos. Environ. 41, 7987–7993.

Kawashima, S., Thibaudon, M., Matsuda, S., Fujita, T., Lemonis, N., Clot, B., Oliver, G., 2017. Automated pollen monitoring system using laser optics for observing seasonal changes in the concentration of total airborne pollen. Aerobiologia 33, 351–362.

Kottek, M., Grieser, J., Beck, C., Rudolf, B., Rubel, F., 2006. World map of the Köppen-Geiger climate classification updated. Meteorol. Z. 15, 259–263.

Lake, I.R., Jones, N.R., Agnew, M., Goodess, C.M., Giorgi, F., Hamaoui-Laguel, L., Semenov, M.A., Solomon, F., Storkey, J., Vautard, R., Epstein, M.M., 2017. Climate change and future pollen allergy in Europe. Environ. Health Perspect. 125, 385–391.

Lieberherr, G., Auderset, K., Calpini, B., Clot, B., Crouzy, B., Gysel-Beer, M., Konzelmann, T., Manzano, J., Mihajlovic, A., Moallemi, A., O'connor, D., Sikoparija, B., Sauvageat, E., Tummon, F., Vasilatou, K., 2021. Assessment of real-time bioaerosol particle counters using reference chamber experiments. Atmos. Meas. Tech. 14, 7693–7706.

Maya-Manzano, J.M., FernÁndez-RodrÍguez, S., Silva-Palacios, I., Gonzalo-Garijo, Á., Tormo-Molina, R., 2018. Comparison between two adhesives (silicone and petroleum jelly) in hirst pollen traps in a controlled environment. Grana 57 (1–2), 137–143. https://doi.org/10.1080/00173134.2017.1319973.

Milic, A., Addison-Smith, B., Jones, P.J., Beggs, P.J., Erbas, B., Davies, J.M., 2019. Quality control of pollen identification and quantification exercise for the AusPollen Aerobiology Collaboration Network: a pilot study. Aerobiologia 36, 83–87. https://doi.org/10.1007/s10453-019-09580-4.

Mishchenko, M.I., Hovenier, J.W., Travis, L.D., 2000. Light scattering by nonspherical particles: theory, measurements, and applications. Meas. Sci. Technol. 11. Academic Press, p. 1827 ISBN: 9780124986602.

O'Connor, D., Healy, D., Hellebust, S., Buters, J., Sodeau, J., 2014. Using the WIBS-4 (Waveband Integrated Bioaerosol Sensor) technique for the on-line detection of pollen grains. Aerosol Sci. Technol. 48, 341–349.

Oteros, J., Galán, C., Alcázar, P., Domínguez-Vilches, E., 2013. Quality control in biomonitoring networks, Spanish Aerobiology Network. Sci. Total Environ. 443, 559–565. https://doi.org/10.1016/j.scitotenv.2012.11.040.

Oteros, J., Orlandi, F., García-Mozo, H., Aguilera, F., Dhiab, A.ben, Bonofiglio, T., Abichou, M., Ruiz-Valenzuela, L., Fornaciari, M., Galán, C., 2014. Better prediction of Mediterranean olive production using pollen-based models. Agron. Sustain. Dev. 34, 685–694.

Oteros, J., Pusch, G., Weichenmeier, I., Heimann, U., Möller, R., Röseler, S., Traidl-Hoffmann, C., Schmidt-Weber, C., Buters, J.T.M., 2015. Automatic and online pollen monitoring. Int. Arch. Allergy Immunol. 167, 158–166.

Oteros, J., Buters, J., Laven, G., Röseler, S., Wachter, R., Schmidt-Weber, C., Hofmann, F., 2017. Errors in determining the flow rate of Hirst-type pollen traps. Aerobiologia 33, 201–210.

Oteros, J., Weber, A., Kutzora, S., Rojo, J., Heinze, S., Herr, C., Gebauer, R., Schmidt-Weber, C.B., Buters, J.T.M., 2020. An operational robotic pollen monitoring network based on automatic image recognition. Environ. Res. 191, 110031.

Plaza, M.P., Kolek, F., Leier-wirtz, V., Brunner, J.O., 2022. Detecting airborne pollen using an automatic, real-time monitoring system: evidence from two sites. Int. J. Environ. Res. Public Health 19 (4), 2471.

R Core Team, 2021. R: A Language and Environment for Statistical Computing.

Razmovski, V., O'meara, T., Hjelmroos, M., Marks, G., Tovey, E., 1998. Adhesive tapes as capturing surfaces in Burkard sampling. Grana 37, 305–310.

Rojo, J., Oteros, J., Pérez-Badia, R., Cervigón, P., Ferencova, Z., Gutiérrez-Bustillo, A.M., Bergmann, K.C., Oliver, G., Thibaudon, M., Albertini, R., Rodríguez-De la Cruz, D., Sánchez-Reyes, E., Sánchez-Sánchez, J., Pessi, A.M., Reiniharju, J., Saarto, A., Calderón, M.C., Guerrero, C., Berra, D., Bonini, M., Chiodini, E., Fernández-González, D., García, J., Trigo, M.M., Myszkowska, D., Fernández-Rodríguez, S., Tormo-Molina, R., Damialis, A., Kolek, F., Traidl-Hoffmann, C., Severova, E., Caeiro, E., Ribeiro, H., Magyar, D., Makra, L., Udvardy, O., Alcázar, P., Galán, C., Borycka, K., Kasprzyk, I., Newbigin, E., Adams-Groom, B., Apangu, G.P., Frisk, C.A., Skjøth, C.A., Radišić, P., Šikoparija, B., Celenk, S., Schmidt-Weber, C.B., Buters, J., 2019a. Near-ground effect of height on pollen exposure. Environ. Res. 174, 160–169.

Rojo, J., Picornell, A., Oteros, J., 2019b. AeRobiology: the computational tool for biological data in the air. Methods Ecol. Evol. 10, 1371–1376.

Rojo, J., Picornell, A., Oteros, J., Werchan, M., Werchan, B., Bergmann, K.-C., Smith, M., Weichenmeier, I., Schmidt-Weber, C., Buters, J., 2021a. Consequences of climate change on airborne pollen in Bavaria,Central Europe. Reg. Environ. Chang. 21, 9. https://doi.org/10.1007/s10113-020-01729-z.

Rojo, J., Oteros, J., Picornell, A., Maya-Manzano, J., Damialis, A., Zink, K., Werchan, M., Werchan, B., Smith, M., Menzel, A., Traidl-Hoffmann, C., Bergmann, K.-C., Schmidt-Weber, C., Buters, J., 2021b. Effects of future climate change on birch pollen exposure. Glob. Chang. Biol. 27, 5934–5949.

Santarpia, J.L., Ratnesar-Shumate, S., Gilberry, J.U., Quizon, J.J., 2013. Relationship between biologically fluorescent aerosol and local meteorological conditions. Aerosol Sci. Technol. 47 (6), 655–661. https://doi.org/10.1080/02786826.2013.781263.

Šaulienė, I., Šukienė, L., Daunys, G., Valiulis, G., Vaitkevičius, L., Matavulj, P., Brdar, S., Panic, M., Sikoparija, B., Clot, B., Crouzy, B., Sofiev, M., 2019. Automatic pollen recognition with the rapid-E particle counter: the first-level procedure, experience and next steps. Atmos. Meas. Tech. 12, 3435–3452.

Sauvageat, E., Zeder, Y., Auderset, K., Calpini, B., Clot, B., Crouzy, B., Konzelmann, T., Lieberherr, G., Tummon, F., Vasilatou, K., 2020. Real-time pollen monitoring using digital holography. Atmos. Meas. Tech. 13, 1539–1550.

Šikoparija, B., 2020. Desert dust has a notable impact on aerobiological measurements in Europe. Aeolian Res. 47, 100636.

Sikoparija, B., Pejak-Šikoparija, T., Radišić, P., Smith, M., Galan, C., 2011. The effect of changes to the method of estimating the pollen count from aerobiological samples. J. Environ. Monit. 13, 384–390.

Sikoparija, B., Galán, C., Smith, M., Abramidze, T., Adams-Groom, B., Albertini, R., Anelli, P., Bastl, K., Bigagli, V., Bonini, M., Bócsi, E., Bucher, E., Caeiro, E., Celenk, S., Cerovac, Chłopek, K., Cislaghi, G., Clot, B., Cortonesi, B., Cristofori, A., Dahl, A., della Bella, V., Dupuy, N., Dušička, J., Ferro, R., Flori, C., Graber, M.J., Hrastovćak, S., Ianovici, N., Józsa, E., Kasprzyk, I., Kmenta, M., Kofler, V., Magyar, D., Mányoki, G., Maya Manzano, J.M., Myszkowska, D., Nowak, M., Oliver, G., Paganoni, B., Palamarchuk, O., Parati, S., Pashley, C., Pini, A., Piotrowska, K., Prentović, M., Rachoud, A.M., Radišić, P., Rapp Benito, A., Rodinkova, V., Russo, M., Sallin, C., Satchwell, J., Sindt, C., Smith, M., Szymanska, A., Šaulienė, I., Ščevková, J., Šikoparija, B., Tassan Mazzocco, F., Testoni, C., Tomičić Žabčić, V., Udvardy, O., Ugolotti, M., Vadassy, R., Vannini, J., Vecenaj, A., Velasco-Jiménez, M.J., Verardo, P., Viola, M.C., Vuillemin, F., Zemmer, F., 2017. Pollen-monitoring: between analyst proficiency testing. Aerobiologia 33, 191–199.

Simonyan, K., Zisserman, A., 2015. Very deep convolutional networks for large-scale image recognition. 3rd International Conference on Learning Representations, ICLR 2015. Conference track Proceedings. Code 149801.

Smith, M., Oteros, J., Schmidt-Weber, C., Buters, J.T.M., 2019. An abbreviated method for the quality control of pollen counters. Grana 58 (3), 185–190. https://doi.org/10.1080/00173134.2019.1570327.

Sofiev, M., Sofieva, S., Palamarchuk, J., Sauliene, I., Kadantsev, E., Atanasova, N., Fatahi, Y., Kouznetsov, R., Kuula, J., Noreikaite, A., Peltonen, M., Pihlajam, T., Saarto, A., Svirskaite, J., Toiviainen, L., Tyuryakov, S., Sukiene, L., Asmi, E., Bamford, D., Hyv, A., Karppinen, A., 2022. Bioaerosols in the atmosphere at two sites in Northern Europe in spring 2021: outline of an experimental campaign. Environ. Res. 214 (Part 2), 113798.

Tešendić, D., Boberić Krstićev, D., Matavulj, P., Brdar, S., Panić, M., Minić, V., Šikoparija, B., 2020. RealForAll: real-time system for automatic detection of airborne pollen. Enterp.Inf. Syst. 16 (5), 1793391.

Tharwat, A., Gaber, T., Ibrahim, A., Hassanien, A.E., 2017. Linear discriminant analysis: a detailed tutorial. AI Commun. 30, 169–190.

Thibaudon, M., Šikoparija, B., Oliver, G., Smith, M., Skjøth, C.A., 2014. Ragweed pollen source inventory for France – the second largest centre of Ambrosia in Europe. Atmos. Environ. 83, 62–71.

Tormo, R., Silva, I., Gonzalo, Á., Moreno, A., Pérez, R., Fernández, S., 2011. Phenological records as a complement to aerobiological data. Int. J. Biometeorol. 55, 51–65.

Triviño, M.M., Maya-Manzano, J.M., Tummon, F., Clot, B., Grewling, Ł., Schmidt-Weber, C., Buters, J., 2023. Resistance free flow adjustment of Hirst-type pollen traps reduces variability between traps. Aerobiologia (Submitted).

Tummon, F., Adamov, S., Clot, B., Crouzy, B., Gysel Beer, M., Kawashima, S., Lieberrherr, G., Manzano, J., Markey, E., Moallemi, A., Connor, D.O., 2021. A first evaluation of multiple automatic pollen monitors run in parallel. Aerobiologia https://doi.org/10.1007/s10453-021-09729-0.

Tummon, F., Bruffaerts, N., Celenk, S., Choël, M., Crouzy, B., Galán, C., Gilge, S., Hajkova, L., Mokin, V., O'Connor, D., Rodinkova, V., Sauliene, I., Šikoparija, B., Sofiev, M., Sozinova, O., Tesendic, D., Vasilatou, K., 2022. Towards standardisation of automatic pollen and fungal spore monitoring: best practises and guidelines. Aerobiologia https://doi.org/10.1007/s10453-022-09755-6.

Wickham, H., Averick, M., Bryan, J., Chang, W., McGowan, L.D., François, R., Grolemund, G., Hayes, A., Henry, L., Hester, J., Kuhn, M., Pedersen, T.L., Miller, E., Bache, S.M., Müller, K., Ooms, J., Robinson, D., Seidel, D.P., Spinu, V., Takahashi, K., Vaughan, D., Wilke, C., Woo, K., Yutani, H., 2019. Welcome to the tidyverse. J.Open Source Softw. 4, 1686.

World Allergy Organization, 2013. WAO White Book on Allergy: Update 2013. World Allergy Organization, Milwaukee, WI.

Zhang, Y., Steiner, A.L., 2022. Projected climate-driven changes in pollen emission season length and magnitude over the continental United States. Nat. Commun. 13, 1234.

Ziska, L.H., Makra, L., Harry, S.K., Bruffaerts, N., Hendrickx, M., Coates, F., Saarto, A., Thibaudon, M., Oliver, G., Damialis, A., Charalampopoulos, A., Vokou, D., Heiðmarsson, S., Guðjohnsen, E., Bonini, M., Oh, J.W., Sullivan, K., Ford, L., Brooks, G.D., Myszkowska, D., Severova, E., Gehrig, R., Ramón, G.D., Beggs, P.J., Knowlton, K., Crimmins, A.R., 2019. Temperature-related changes in airborne allergenic pollen abundance and seasonality across the northern hemisphere: a retrospective data analysis. Lancet Planet.Health 3, e124–e131.